Direct Observation of the Kinetic Acidities of Transient Aromatic Cation Radicals. The Mechanism of Electrophilic Side-Chain Nitration of the Methylbenzenes

J. M. Masnovi,[†] S. Sankararaman,[‡] and J. K. Kochi*[,‡]

Contribution from the Department of Chemistry, University of Houston, University Park, Houston, Texas 77204-5641, and the Department of Chemistry, Cleveland State University, Cleveland, Ohio 44115. *Received August 15, 1988*

Abstract: The transient cation radicals $ArCH_3^{\bullet+}$ are spontaneously generated by the 532-nm excitation of the charge-transfer complexes $[ArCH_3,C(NO_2)_4]$ with a 10-ns laser pulse. The decay kinetics of the spectral transients in the presence of added base establish the kinetic acidities (k_H) for various methylarene cation radicals with different pyridines and trinitromethide. Such a proton transfer from $ArCH_3^{\bullet+}$ proceeds with a deuterium kinetic isotope effect of $k_H/k_D \cong 3$. Side-chain nitration of hexamethylbenzene (HMB) is shown to proceed in high yields via the intimate triad of reactive fragments II, $[HMB^{\bullet+},NO_2,C(NO_2)_3^-]$, that is produced upon the charge-transfer excitation. The subsequent annihilation of the reactive triad II occurs via a rapid succession of bimolecular steps involving either (i) the initial ion-pair collapse of $[HMB^{\bullet+},C(NO_2)_3^-]$ by proton transfer, as shown in Scheme VI, or (ii) the alternative sequence with the initial ion–radical collapse of $[HMB^{\bullet+},NO_2^{\bullet}]$ by homolytic coupling, as shown in Scheme VII. The marked variations of k_H/k_D with solvent polarity and added innocuous salt ($Bu_4N^+ClO_4^-$), as reflected in ion-pair separation and the "special" salt effect, serve to effectively distinguish these pathways. The direct bearing of Schemes VI and VII on the mechanism of the thermal (adiabatic) nitration of methylarene side chains with nitric acid is delineated.

Electrophilic substitution of aromatic hydrocarbons (i.e., electrophilic aromatic substitution) represents one of the cornerstones of synthetic and mechanistic organic chemistry.[1] Nonetheless there exists a bewildering and curious variety of accompanying side reactions that in some cases can be highly competitive, such as ipso replacement, alkyl rearrangement, biaryl coupling, side-chain substitution, and oxidation.[2] These processes are often euphemistically referred to as "nonconventional" processes since it is not clear whether they all converge to a common mechanistic origin.[3] Among the diverse reaction types, the electrophilic replacement of a benzylic hydrogen is an especially intriguing transformation, occurring as it does at a saturated (sp^3) carbon site. For example, the nitration of durene carried out under the usual conditions for electrophilic aromatic nitrations,[4] namely nitric acid in acetic anhydride, leads to substantial amounts of the side chain substituted α-nitrodurene, in addition to the expected 3-nitrodurene.[5] Several explanations have been put forth to

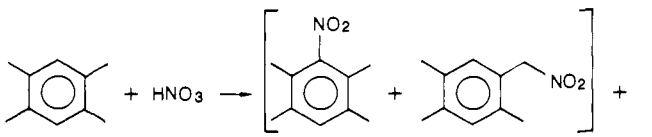

(1)

account for such a bifurcation of reaction pathways to favor the side-chain nitration. Among these possibilities, two are distinctive mechanisms, namely, (a) electrophilic addition–elimination to generate a methylenecyclohexadiene intermediate followed by sigmatropic rearrangement,[6] e.g.

Scheme I

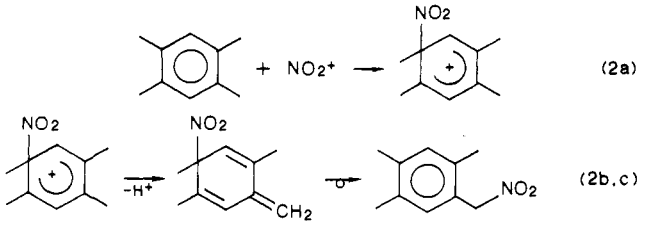

and (b) electron transfer to form an aromatic cation radical followed by deprotonation,[7] e.g.

Scheme II

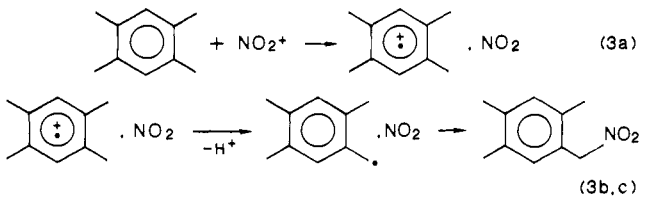

The viability of Scheme I has recently been shown in the spectral (NMR) observation of the triene (eq 2b) at low temperatures and its subsequent rearrangement.[8] By the same token, support for Scheme II derives from the behavior of aromatic cation radicals generated by a variety of chemical, photochemical, and electrochemical methods for electron detachment that lead to deprotonation and benzylic substitution.[9-12] Since aromatic cation

[†] Cleveland State University.
[‡] University of Houston.

(1) See, e.g., Carey, F. A.; Sundberg, R. J. *Advanced Organic Chemistry*, Parts A and B; 2nd ed.; Plenum: New York, 1984. March, J. *Advanced Organic Chemistry, Reactions, Mechanisms and Structure*; 2nd ed.; McGraw-Hill: New York, 1986.
(2) Baciocchi, E.; Illuminati, G. *Prog. Phys. Org. Chem.* **1967**, *5*, 1.
(3) Hartshorn, S. R. *Chem. Soc. Rev.* **1974**, *3*, 167.
(4) Schofield, K. *Aromatic Nitration*; Cambridge University Press: Cambridge, 1980.
(5) Blackstock, D. J.; Fischer, A.; Richards, K. E.; Wright, G. J. *Aust. J. Chem.* **1973**, *26*, 775. In addition, 2,3,5,6-tetramethylphenyl acetate (33%), 2,4,5-trimethylbenzyl alcohol (6%), and 2,4,5-trimethylbenzaldehyde (3%) are produced.
(6) (a) Astolfi, R.; Baciocchi, E.; Illuminati, G. *Chim. Ind. (Milan)* **1971**, *33*, 1153. (b) The nitronium ion is depicted merely as a convenience since other electrophilic nitrating agents could be involved.
(7) Suzuki, H. *Chem. Lett.* **1987**, 891.
(8) Fischer, A.; Goel, A. *J. Chem. Soc., Chem. Commun.* **1988**, 526.
(9) (a) Beletskaya, I. P.; Makhon'kiv, D. I. *Russ. Chem. Rev. (Engl. Transl.)* **1981**, *50*, 1007. (b) Sheldon, R. A.; Kochi, J. K. *Metal Catalyzed Oxidation of Organic Compounds*; Academic Press: New York, 1981.
(10) (a) Hammerich, O.; Parker, V. D. *Adv. Phys. Org. Chem.* **1984**, *20*, 55. (b) Yoshida, K. *Electrooxidation in Organic Chemistry*; Wiley-Interscience: New York, 1984. (c) Nyberg, K. In *Encyclopedia of Electrochemistry of the Elements*; Bard, A. J., Lund, H., Eds.; Marcel Dekker: New York, 1978; Vol. XI, Chapter IX, pp 43-70. Eberson, L.; Nyberg, K. *Acc. Chem. Res.* **1973**, *6*, 106.
(11) (a) Kavarnos, G. J.; Turro, N. J. *Chem. Rev.* **1986**, *86*, 401. (b) Marino, P. S.; Stavinoha, J. L. In *Synthetic Organic Photochemistry*; Horspool, W. M., Ed.; Plenum Press: New York, 1984; Chapter 3, pp 145-257. (c) Mattes, S. L.; Farid, S. In *Organic Photochemistry*; Padwa, A., Ed.; Marcel Dekker: New York, 1983; Vol. 6, Chapter 4, pp 233-326. (d) Nagakura, S. In *Excited States*; Lim, E. C., Ed.; Academic Press: New York, 1975; Vol. 5, pp 321-83. (e) Kaiser, E. T.; Kevan, L. *Radical Ions*; Interscience: New York, 1968. (f) Lewis, F. D. *Acc. Chem. Res.* **1986**, *19*, 401.

0002-7863/89/1511-2263$01.50/0

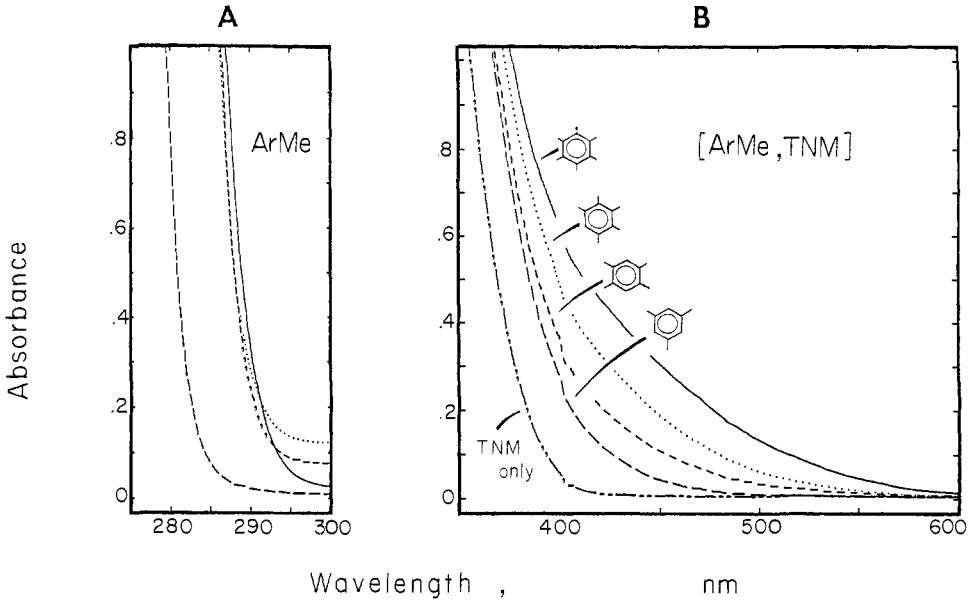

Figure 1. Electronic absorption spectra of 0.05 M methylarenes in acetonitrile (left) and in the presence of 0.1 M tetranitromethane (right): HMB (—), PMB (···), DUR (- -), and MES (– –), together with the absorption cutoff of 0.1 M TNM alone (– · –).

radicals ($ArCH_3^{\bullet+}$, eq 3b) also react directly at nuclear positions,[13] these reactive intermediates offer a common pathway to unify the electrophilic side-chain nitration (e.g., α-nitrodurene in eq 3) with aromatic nuclear nitration (3-nitrodurene) via a *single* mechanistic theme. In a more general vein the rate-limiting electron transfer in Scheme II is also directly relevant to other competitive side reactions in aromatic nitration leading to oxynitration, acyloxylation, alkoxylation, biaryl coupling, quinones, etc.[14]

Although the study of such reactive intermediates as aromatic cation radicals has heretofore been based on largely indirect methods (mostly by relying on kinetics analyses), it is now possible to examine them by direct, time-resolved spectroscopic methods.[15] Thus we recently demonstrated that electron transfer is induced by the charge-transfer (CT) irradiation of electron donor–acceptor or EDA complexes.[15] As applied to aromatic nitration, the requisite aromatic cation radical for Scheme II should be spontaneously produced from the CT activation ($h\nu_{CT}$) of appropriate aromatic EDA complexes with tetranitromethane, as previously established for anthracene (An) donors below.[16]

Scheme III

$$An + C(NO_2)_4 \rightleftharpoons An,C(NO_2)_4 \quad (4)$$

$$An,C(NO_2)_4 \xrightarrow{h\nu_{CT}} \underset{I}{[An^{\bullet+},NO_2^{\bullet},C(NO_2)_3^-]} \quad (5)$$

Indeed the brackets in eq 5 denote the solvent-caged triad of reactive species I that is akin to the intimate ion–radical pair presented in eq 3a.[17] As such, the chemical behavior of I should provide direct access to those factors affecting the dichotomy in electrophilic nitration between nuclear and side-chain substitution. Accordingly, our ultimate objective in this study is to test the viability of Scheme III for various methylarenes like durene which are capable of both nuclear and side-chain nitration, as shown in eq 1. We begin by establishing the critical ion–radical pair as the reactive intermediate from the charge-transfer excitation of EDA complexes (Scheme III) with the established series of methylarenes: hexamethylbenzene, pentamethylbenzene, durene, and mesitylene.

Results

I. Spontaneous Formation of Charge-Transfer Complexes of Methylarenes. Solutions of various methylarenes in acetonitrile immediately took on a strong coloration when mixed with tetranitromethane (TNM). The colors progressively varied from yellow to orange to red with increasing numbers of methyl substituents on the $ArCH_3$ in the following order: mesitylene (MES), durene (DUR), pentamethylbenzene (PMB), and hexamethylbenzene (HMB). The accompanying changes in the electronic absorption spectra are illustrated in Figure 1 in comparison with the spectra of the methylarenes themselves. Although the spectral maxima were obscured by the low-energy tail absorption of the TNM acceptor, the unmistakable red shifts in Figure 1B clearly paralleled the decrease in the ionization potentials of the methylarenes [MES (8.42 eV), DUR (8.05 eV), PMB (7.92 eV), and HMB (7.85 eV)[18]]. As such, the new absorptions accorded with the charge-transfer bands of electron donor–acceptor complexes of the type described by Mulliken,[19] i.e.

$$ArCH_3 + C(NO_2)_4 \overset{K}{\rightleftharpoons} [ArCH_3,C(NO_2)_4] \quad (6)$$

Judging by the changes in the CT absorbance with increasing amounts of either the methylarene or TNM, we concluded that the formation constant K in eq 6 was small ($K < 1\ M^{-1}$).[16] Thus the methylarene complexes with TNM, like those with TCNE,[20] were derived from weak ground-state interactions.[21] The presence of added lithium perchlorate and pyridine bases that were pertinent to this study (vide infra) did not have any noticeable effect on

(12) (a) Albini, A.; Spreti, S. J. *Chem. Soc., Perkin Trans. 2* **1987**, 1175. (b) Arnold, D. R.; Mines, S. A. *Can. J. Chem.* **1987**, *65*, 2312. (c) Minisci, F.; Vismara, E.; Morini, G.; Fontana, F.; Levi, S.; Serravalle, M. *J. Org. Chem.* **1986**, *51*, 476. (d) Green, M. M.; Mielbe, S. L.; Mukhopadhyay, T. *J. Org. Chem.* **1984**, *49*, 1276. (e) Sehested, K.; Holcman, J. *J. Phys. Chem.* **1978**, *82*, 651.

(13) (a) Parker, V. D.; Tilset, M. *J. Am. Chem. Soc.* **1987**, *109*, 2521. (b) Brandys, M.; Sassoon, R. E.; Rabani, J. *J. Phys. Chem.* **1987**, *91*, 953. (c) Evans, J. F.; Blount, H. N. *J. Am. Chem. Soc.* **1978**, *100*, 4191.

(14) Suzuki, H. *Synthesis* **1977**, 217.

(15) (a) Masnovi, J. M.; Kochi, J. K. *J. Am. Chem. Soc.* **1985**, *107*, 6781. (b) Lau, W.; Kochi, J. K. *J. Org. Chem.* **1986**, *51*, 1801.

(16) (a) Masnovi, J. M.; Kochi, J. K.; Hilinski, E. F.; Rentzepis, P. M. *J. Am. Chem. Soc.* **1986**, *108*, 1126. (b) Masnovi, J. M.; Kochi, J. K. *J. Org. Chem.* **1985**, *50*, 5245. (c) Compare also Gorodyskii, B. A.; Perekalin, V. V. *Dokl. Akad. Nauk SSSR, Ser. Chim.* **1967**, *173*, 123. (d) Hammick, D. L.; Young, R. P. *J. Chem. Soc.* **1936**, 1463.

(17) Masnovi, J. M.; Kochi, J. K. *J. Am. Chem. Soc.* **1985**, *107*, 7880.

(18) Howell, J. O.; Goncalves, J. M.; Amatore, C.; Klasinc, L.; Wightman, R. M.; Kochi, J. K. *J. Am. Chem. Soc.* **1984**, *106*, 3968.

(19) Mulliken, R. S. *J. Am. Chem. Soc.* **1952**, *74*, 811. Mulliken, R. S.; Person, W. B. *Molecular Complexes: A Lecture and Reprint Volume*; Wiley: New York, 1969.

(20) Masnovi, J. M.; Hilinski, E. F.; Rentzepis, P. M.; Kochi, J. K. *J. Phys. Chem.* **1985**, *89*, 5387.

(21) Foster, R. *Organic Charge-Transfer Complexes*; Academic Press: New York, 1969.

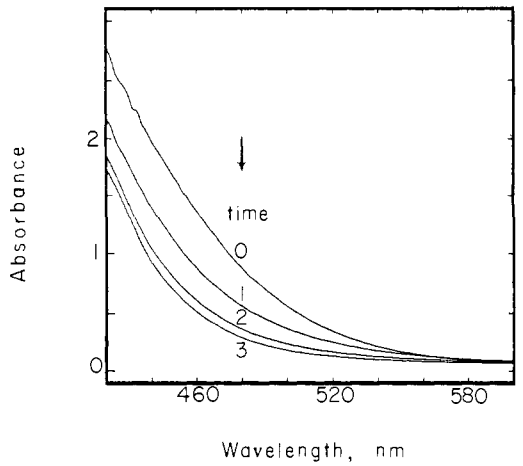

Figure 2. Typical bleaching of the charge-transfer band upon actinic irradiation at $\lambda > 425$ nm, as shown for a solution of 0.1 M PMB and 0.5 M TNM in acetonitrile after (top to bottom) 0, 1, 2, and 3 h.

either the intensity or the position of the CT absorption bands.

II. Charge-Transfer Activation of Methylarene EDA Complexes. Products and Stoichiometry. The EDA complexes of methylarenes ($ArCH_3$) and tetranitromethane in eq 6 persisted unchanged for several days if these solutions were carefully protected. However, upon the deliberate exposure to actinic light, the colored solutions were uniformly bleached. As a result, the subsequent photochemical studies were always carried out with filtered light (usually with $\lambda > 425$ nm) to ensure the selective excitation of only the CT bands (compare Figure 1, parts A and B) of the various methylarene complexes.[22]

The course of the charge-transfer photochemistry was followed by measuring either the disappearance of the methylarene absorbance (Figure 1A) or the bleaching of the colored charge-transfer band, as illustrated in Figure 2 for a typical methylarene EDA complex. The subsequent analysis of the photolysate revealed the presence of two types of aromatic products.[23] On one hand, mesitylene afforded the nuclear nitration product 2-nitromesitylene in 65% yield according to the stoichiometry:

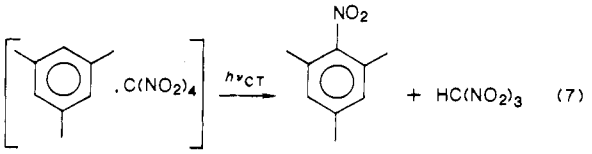

The residual trinitromethyl moiety was identified as nitroform by extraction of the crude reaction mixture dissolved in ether with water. Under the same conditions, the CT irradiation of the hexamethylbenzene complex yielded the side chain nitration product pentamethyl-α-nitrotoluene in 82% yield, i.e.

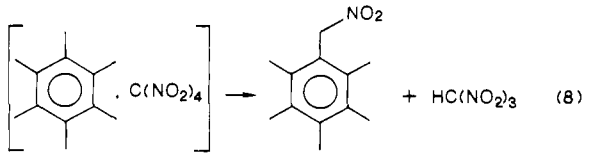

The charge-transfer photochemistry of [$ArCH_3$,TNM] complexes leading to the aromatic products in eq 7 and 8 will be referred to hereafter as *charge-transfer nitration* as directed to nuclear and side-chain substitution, respectively. Although these stoichiometries represented the principal course of CT nitration, the formation of small but discrete amounts of aromatic byproducts was revealing. For example, the trinitromethyl moiety was

Table I. Substitution Products from the Charge-Transfer Activation of Methylarene EDA Complexes[a]

methylarene ($ArCH_3$)	side-chain substitution[b]		nuclear substitution[b,c]		$HC(NO_2)_3$, %[d]
	$ArCH_2NO_2$	$ArCH_2T$	$Ar'NO_2$	Ar'T	
(MES)	0	0	65	10[e]	56
(DUR)	72	10[f]	21	<1[g]	92
(PMB)	91	1	6	0	98
(HMB)	82	14	0	0	80

[a] In 3.0mL of acetonitrile containing 0.1 M $ArCH_3$ and 0.5 M TNM, by actinic irradiation at $\lambda > 425$ nm. [b] From ^1H NMR and GC analysis (see the Experimental Section). T = $C(NO_2)_3$. Numbers refer to yield (%) based on the amount of $ArCH_3$ recovered. [c] Ar' = MeAr(−H). [d] Total nitroform. [e] As mesitoic acid from hydrolysis. [f] Includes 5% of 2,4,5-trimethylbenzaldehyde. [g] As duroic acid from hydrolysis (see the Experimental Section).

partially diverted to the product of nuclear substitution of mesitylene, i.e.

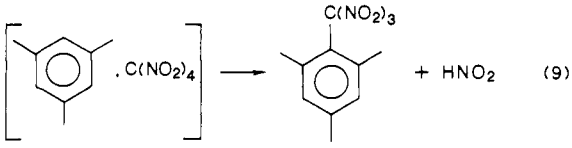

and to the product of side-chain substitution of hexamethylbenzene:[23,24]

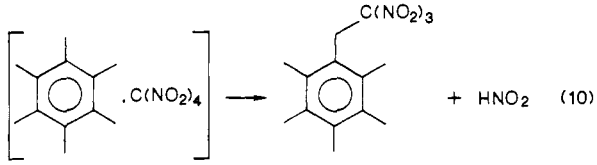

Nuclear nitration and trinitromethylation in eq 7 and 9 together accounted for essentially all of the mesitylene consumed in the course of CT activation, as listed in Table I. Likewise, the side-chain nitration and trinitromethylation in eq 8 and 10, respectively, together constituted the complete material balance for the disappearance of hexamethylbenzene. It was thus noteworthy that durene, which intervenes between HMB and MES, yielded a mixture of aromatic products derived from both side-chain and nuclear substitution in a ratio of approximately 3:1, as outlined in Table I.[23] Moreover, pentamethylbenzene also underwent side-chain nitration and to a lesser degree nuclear nitration.

III. Quantum Yields for Charge-Transfer Nitration of Methylarenes. The photochemical efficiency of the side-chain nitration of hexamethylbenzene (HMB), pentamethylbenzene (PMB), and durene (DUR) in acetonitrile was measured with a Reinecke salt actinometer. Quantitative measurements were carried out in 1-cm quartz cells, with the irradiation of the solutions effected by monochromatic light obtained upon the passing of the output from a 450-W high pressure xenon lamp through a water filter followed by an interference filter (10-nm bandpass). The interference filter for HMB and PMB was set at 505 nm, and for DUR a 450-nm interference filter was used. The absorbances of the actinometry solutions at these wavelengths were always greater than 1.5, and corrections were made for the transmitted light. After irradiation, the photolysates containing the unreacted

(22) The use of such filtered light obviated any complication from the photoinduced homolysis of TNM. See: Frank, A. J.; Graetzel, M.; Henglein, A. *Ber. Bunsenges. Phys. Chem.* **1976**, *80*, 593. Isaacs, N. S.; Abed, O. H. *Tetrahedron Lett.* **1982**, *23*, 2799.

(23) See the Experimental Section for details.

(24) (a) The aromatic product in eq 9 was identified as mesitoic acid owing to its rapid hydrolysis.[25] (b) For the formation of nitrous acid in eq 9 and 10, see ref 25.

(25) Sankararaman, S.; Haney, W. A.; Kochi, J. K. *J. Am. Chem. Soc.* **1987**, *109*, 5235.

Table II. Effect of Solvent and Additives on the Charge-Transfer Activation of EDA Complexes[a]

$ArCH_3$	solvent	additive[b]	product distribution (%)[c]				
			$ArCH_2NO_2$	$ArCH_2T$	$Ar'NO_2$	Ar'T	$HC(NO_2)_3$
HMB	MeCN	$LiClO_4$	81[d]	17			146
	MeCN	Bu_2py	69[e]	36[f]			-
	CH_2Cl_2	0	45	50[g]			-
	n-C_6H_{14}	0	40	20[h]			-
PMB	MeCN	$LiClO_4$	50	17[i]	19	0	65
	MeCN	Bu_2py	50	10[j]	20	0	-
DUR	MeCN	$LiClO_4$	50	25[k]	20	5	83
	MeCN	TBAF	75	7[l]	20	-	-
	MeCN	Bu_2py	65	28[m]	4	-	-
	CH_2Cl_2	0	20	25	20	5	-
MES	MeCN	Bu_2py	0	0	50	<5[n]	
	CH_2Cl_2	0	0		40	50[n]	

[a] In 3.0 mL of solvent containing 0.1 M $ArCH_3$ and 0.5 M TNM by irradiation at $\lambda > 425$ nm. [b] Either 0.1 M $LiClO_4$ or Bu_2py = 0.1 M 2,6-*di-tert*-butylpyridine with 0.1 M $LiClO_4$, or TBAF = 0.1 M n-$Bu_4N^+PF_6^-$. [c] See Table I. [d] Includes 26% of α,β-dinitrohexamethylbenzene. [e] Includes 9% of α,β-dinitro-HMB. [f] Includes 35% of $ArCH_2ONO_2$. [g] Includes 15% of $ArCH_2ONO_2$ and 15% of $ArCH_2ONO$. [h] Includes 10% of $ArCH_2ONO_2$. [i] Includes 12% of 2,3,4,5-$Me_4C_6H(CHO)$ and traces of $ArCH_3$ dimer. [j] Includes 10% of $ArCH_3$ dimer. [k] Includes 20% of 2,4,5-$Me_3C_6H_2CHO$. [l] Includes 6% of 2,4,5-$Me_3C_6H_2CHO$. [m] Includes 13% of 2,4,5-$Me_3C_6H_2CHO$. [n] As mesitoic acid.

arene and the side chain nitration product were analyzed by quantitative gas chromatography with *p*-xylene as the internal standard (see the Experimental Section). The quantum yields for the formation of the side chain nitration products were found to be Φ_p = 0.06, 0.04, and 0.05 for HMB, PMB, and DUR, respectively. Similarly, the quantum yields for the disappearance of the starting arenes were Φ_r = 0.08, 0.043, and 0.053 for HMB, PMB, and DUR, respectively.

IV. Effect of Additives on the Side-Chain versus Nuclear Nitration of Methylarenes. The environmental factors leading to the varying competition between side-chain and nuclear substitution in Table I were examined by carrying out the charge-transfer activation of the same series of EDA complexes in different solvents and with different additives. Table II lists the effects of added salt (lithium perchlorate) and the presence of a pyridine base upon this competition.[26] Of particular importance was the pronounced effect of 2,6-di-*tert*-butylpyridine (DBP) on the relative amounts of nuclear and side chain substitution products of durene. Thus the 21% yield of 3-nitrodurene suffered a sharp drop-off to only 4% (with a concomitant increase in side chain substitution products) when merely 1 equiv of this hindered pyridine base was present during the CT activation of the EDA complex. Therefore a closer, more systematic study of the competition between the side-chain and nuclear substitution of durene was also carried out with 2,6-lutidine (LUT). The results shown in Figure 3 established the inverse relationship between side-chain and nuclear nitration of durene with increasing amounts of 2,6-lutidine—diagnostic of the competition below:

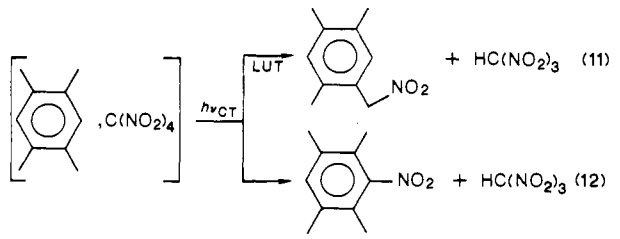

The foregoing environmental effects on the aromatic products (Table II, Figure 3) have identified the critical importance of pyridine bases on the side-chain nitration of methylarenes. In order to trace the source of the pyridine effect, we turned to time-resolved spectroscopy for the identification of the reactive intermediates involved in the CT activation of methylarene EDA complexes, especially with regard to their kinetics behavior in the presence of added pyridine bases.

V. Direct Observation of Methylarene Cation Radicals as the Transient Intermediate in Charge-Transfer Activation of EDA Complexes. The photobleaching of the charge-transfer band (Figure 2) was examined closely by time-resolved spectroscopy using a 10-ns (fwhm) laser pulse. The excitation wavelength of 532 nm corresponded to the second harmonic of a Q-switched Nd^{3+}:YAG laser, and it was optimally suited to excite only the low-energy tails of the CT absorption bands (see Figure 1B). Therefore there was no ambiguity in these time-resolved studies about either the adventitious local excitation of the uncomplexed methylarene (Figure 1A) or the generation of intermediates which did not result from the direct charge-transfer excitation of the EDA complexes.

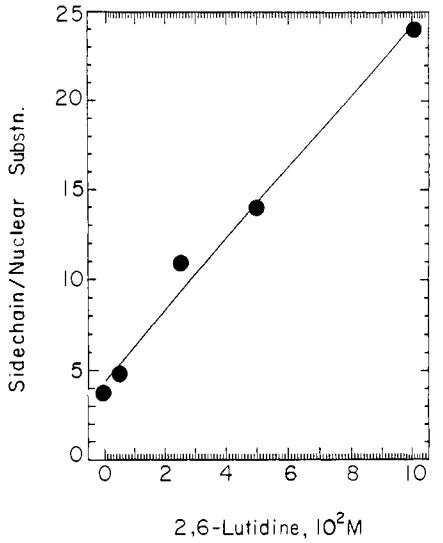

Figure 3. Competition between side-chain and nuclear substitution as a function of added base (lutidine) in the CT nitration of 0.1 M DUR and 0.5 M TNM in acetonitrile at $\lambda > 425$ nm.

The time-resolved spectra obtained from the charge-transfer excitation of the various methylarene EDA complexes always consisted of a characteristic pair of absorption bands, T and C. The higher energy, more intense band T (with λ_{max} consistently at 350 ± 10 nm) was rather persistent, and it was readily ascribed to the trinitromethide anion by comparing its electronic spectrum with that of the authentic salt [n-$Bu_4N^+C(NO_2)_3^-$] showing λ_{max} = 350 nm and ϵ_{350} = 14 000 M^{-1} cm^{-1} in acetonitrile.[17,27] The location of the weaker, transient absorption band C varied with the methylarene, and it was assigned to the cation radical $ArCH_3^{\bullet+}$ as follows. (i) The time-resolved spectrum in Figure 4 (with the transient band at λ_{max} = 495 nm) obtained from the charge-transfer excitation of the hexamethylbenzene EDA complex co-

(26) Among the byproducts listed in Table II, the nitrates, nitrites, aldehydes, and $ArCH_3$ dimers are grouped with side-chain trinitromethylation, and the benzoic acids with nuclear trinitromethylation.[23]

(27) Compare also Kamlet, M. J.; Glover, D. J. *J. Org. Chem.* **1962**, *27*, 537.

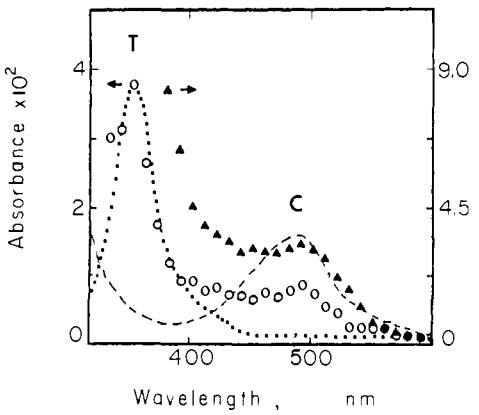

Figure 4. Time-resolved absorption spectra from acetonitrile solutions of 0.05 M HMB and (▲) 0.1 M TNM after 4 μs at λ = 532 nm and (○) 0.01 M TNM after 400 ns at λ = 355 nm excitation. Steady-state spectra of $HMB^{\bullet+}$ (--) and $C(NO_2)_3^-$ (···) are shown for comparison.

incided with the absorption spectrum of $HMB^{\bullet+}$ generated independently by several methods (see dashed curve).[28] (ii) The time-resolved spectra from the charge-transfer excitation of the pentamethylbenzene and durene EDA complexes located the transient band C at λ_{max} = 485 and 440 nm, respectively, in agreement with the absorption spectra of the cation radicals $PMB^{\bullet+}$ and $DUR^{\bullet+}$ generated independently.[29] (iii) The progressive red-shifts in the transient band C of the cation radicals produced from DUR, PMB, and HMB accorded with the theoretical expectations based on the increasing number (and location) of the methyl substituents.[30] (iv) The absorption band C was rapidly quenched by electron transfer from the reducing agent 9,10-diphenylanthracene (DPA), whereas the band T was unaffected (vide infra).

The simultaneous appearance of the ion pairs consisting of $C(NO_2)_3^-$ and $ArCH_3^{\bullet+}$ demonstrates the charge-transfer activation of the methylarene EDA complexes to be the following:

$$\underset{\text{II}}{[ArCH_3,C(NO_2)_4]} \xrightarrow{h\nu_{CT}} [ArCH_3^{\bullet+},C(NO_2)_3^-,NO_2] \quad (13)$$

The presence of NO_2 was obscured in Figure 4 owing to the spectral overlap of the weak, broad continuum spanning the spectral range from 250 nm to beyond 800 nm with the absorptions of the other components.[31] Nonetheless its contribution to II was unmistakable owing to the unambiguous stoichiometries established by eq 7–10. As such, the charge-transfer activation of the methylarene EDA complexes to produce the triad of reactive intermediates in eq 13 is the same as that previously shown with EDA complexes of anthracene donors (Scheme III).[16]

VI. Quenching Kinetics for Methylarene Cation Radicals. The temporal evolution of the time-resolved spectrum emphasized the distinctly different dynamic changes of the absorption bands T and C. For example, the minor diminution of band T indicated that trinitromethide, once formed, remained relatively intact.

Table III. Electron-Transfer Quenching of Methylarene Cation Radicals by 9,10-Diphenylanthracene[a]

methylarene	solvent	λ_{mon},[b] nm	k_{et},[c] 10^{-9} M^{-1} s^{-1}	ΔG_{et},[d] V
HMB	CH_2Cl_2	495	6.5	−0.52
		(660)	(7.1)	
	MeCN	500	7	−0.52
		(660)	(6)	
HEB[e]	CH_2Cl_2	495	7.4	−0.49
		(660)	(7.4)	
PMB	MeCN	470	*g*	−0.65
		(660)	(4)	
DUR	MeCN	450	*g*	−0.72
		(660)	(9)	
NTB[f]	CH_2Cl_2	495	*h*	
		(660)	(6.5)	−0.41

[a] In solutions containing ~5 × 10^{-2} M $ArCH_3$, 0.1 M TNM, ~5 × 10^{-4} M DPA, and either 0.1 M TBAP (CH_2Cl_2) or 0.1 M $LiClO_4$ (MeCN) at 22 °C. [b] Monitoring wavelength of $ArCH_3^{\bullet+}$ or ($DPA^{\bullet+}$). [c] Determined under pseudo-first-order conditions. [d] Driving force = $-\Delta G_{et}$ as described in ref 36. [e] Hexaethylbenzene. [f] 1,2-Dineopentyltetramethylbenzene. [g] Absorbance too small for reliable measurement. [h] Not determined.

Contrastingly, the rapid disappearance of the absorption band C confirmed the highly transient nature of the methylarene cation radical. The marked rate of disappearance of $HMB^{\bullet+}$ is underscored in Figure 5. The examination of [$HMB^{\bullet+}$] at the monitoring wavelength of 500 nm indicated that the decay profile followed second-order kinetics in dichloromethane with the rate constant of 4.3 × 10^6 A^{-1} s^{-1} on the return of the absorbance to the base line (see the Experimental Section).

This kinetics behavior was consistent with the first-formed triad of reactive intermediates being sufficiently long-lived in dichloromethane to allow diffusive separation (a) prior to the second-order recombination (b) in eq 14. Furthermore the slower

$$\underset{\text{II}}{[ArCH_3^{\bullet+},C(NO_2)_3^-,NO_2]} \xrightarrow[[-NO_2]]{(a)} ArCH_3^{\bullet+} + C(NO_2)_3^- \xrightarrow{(b)} \text{etc.} \quad (14)$$

rate of disappearance of the perdeuteriated derivative HMB-d_{18} by a factor of 2.8 suggested a rate-limiting proton transfer, i.e.

$$ArCH_3^{\bullet+} + C(NO_2)_3^- \rightarrow ArCH_2^{\bullet} + HC(NO_2)_3 \quad (15)$$

Such a deprotonation of $HMB^{\bullet+}$ was entirely consistent with the side-chain products derived from hexamethylbenzene, as in Table II. (Note that nitroform exists in solution primarily as trinitromethide owing to the value of pK_a = 0.17.)

The diffusive separation of the reactive intermediates as in eq 14b allowed the interception of the methylarene cation radicals by additives such as electron donors as well as the Brønsted bases described separately below.

A. Quenching of $ArCH_3^{\bullet+}$ by electron donors was deemed to be optimum with 9,10-diphenylanthracene (DPA) owing to its favorable oxidation potential of E_0 = 1.26 V vs SCE.[32] Indeed the presence of as little as 10^{-4} M 9,10-diphenylanthracene during the CT excitation of the hexamethylbenzene EDA complex effectively quenched the absorption band of $HMB^{\bullet+}$ at λ_{max} = 495 nm, as shown in Figure 6. The concomitant appearance of the intense absorption spectrum of the cation radical of diphenylanthracene with the characteristic λ_{max} = 580, 660, and 730 nm[11e] shown in Figure 6 represented the electron-transfer process:

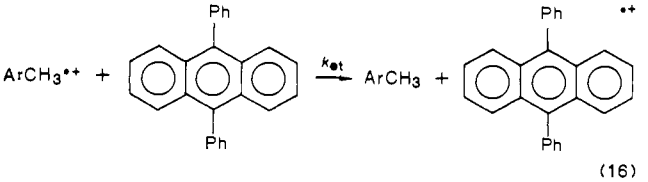

(16)

(28) (a) The dashed curve represents the absorption spectrum of $HMB^{\bullet+}$ generated spectroelectrochemically.[16] Similar absorption spectrum of $HMB^{\bullet+}$ were obtained by Peacock and Schuster, and Teng and Dunbar. (b) Peacock, N.; Schuster, G. B. *J. Am. Chem. Soc.* **1983**, *105*, 3632. (c) Teng, H. H.; Dunbar, R. C. *J. Chem. Phys.* **1978**, *68*, 3133. (d) Preliminary measurements indicate that the extinction coefficient of $HMB^{\bullet+}$ is ϵ_{max} ~ 900 M^{-1} cm^{-1}. Second-order rate constants in units of M^{-1} s^{-1} can be obtained by multiplying the observed rate constants in A^{-1} s^{-1} by ϵ_{max}.

(29) Sankararaman, S.; Kochi, J. K., to be published.

(30) Heilbronner, E.; Maier, J. P. In *Electron Spectroscopy*; Brundle, C. R., Baker, A. D., Eds.; Academic: New York, 1977, Vol. 1, p 205 ff.

(31) (a) For NO_2, see: Gillespie, G. D.; Khan, A. U. *J. Chem. Phys.* **1976**, *65*, 1624. Hall, T. C., Jr.; Blacet, F. E. *J. Chem. Phys.* **1952**, *20*, 1745. (b) The principal absorptions of other possible transients lie below 400 nm; e.g., arenium ions (Koptyug, V. A. *Top. Curr. Chem.* **1984**, *122*, 1), benzylic radicals (Claridge, R. F. C.; Fischer, H. *J. Phys. Chem.* **1985**, *87*, 1960; Branciard-Larcher, C.; Migirdicyan, E.; Baudet, J. *Chem. Phys.* **1973**, *2*, 95), benzylic cations (Hanazaki, I.; Nagakura, S. *Tetrahedron* **1965**, *21*, 2441), and arene dimer cations (Badger, B.; Brocklehurst, B. *Trans. Faraday Soc.* **1969**, *65*, 2582).

(32) Masnovi, J. M.; Seddon, E. A.; Kochi, J. K. *Can. J. Chem.* **1984**, *62*, 2552.

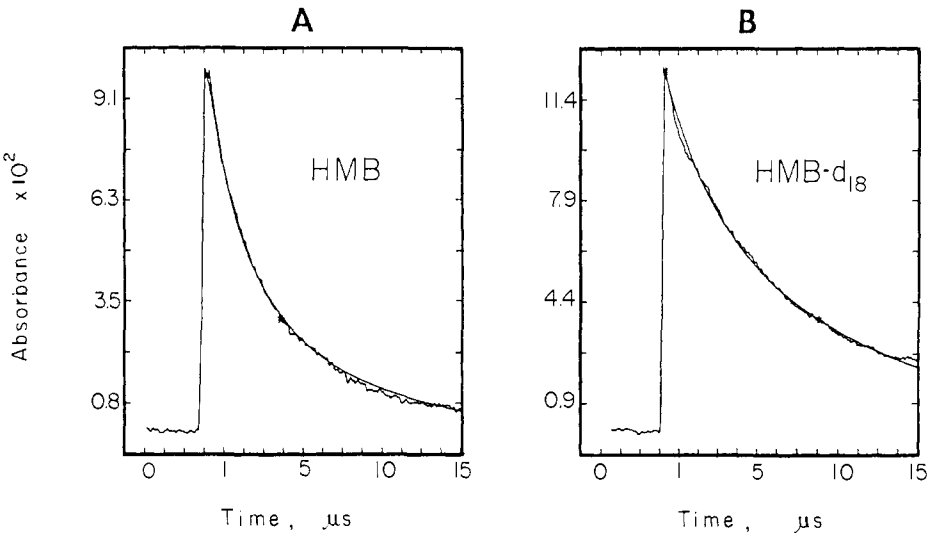

Figure 5. Decay profile of the $HMB^{\bullet+}$ absorbance at 495-nm following the 532-nm excitation of a solution of 0.05 M HMB (left) or HMB-d_{18} (right) together with 0.1 M TNM in dichloromethane at 24 °C. The smooth curves are the computer-fitted least-squares treatment of the data for second-order kinetics.

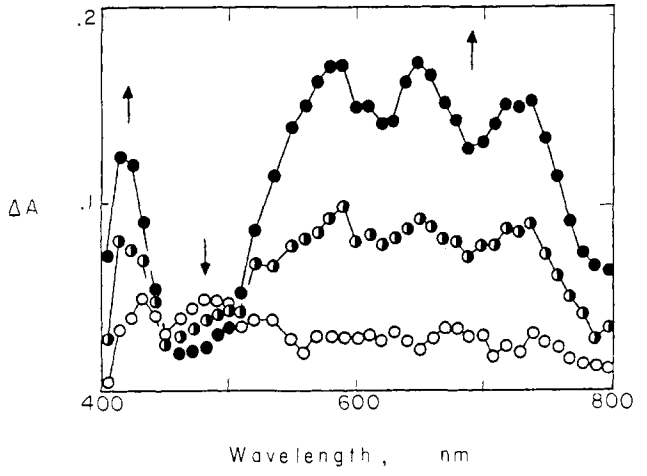

Figure 6. Appearance of $DPA^{\bullet+}$ at 10 (○), 45 (◑), and 300 (●) ns following the 532-nm excitation of a solution of 0.5 M HMB and 0.1 M TNM in dichloromethane containing 1×10^{-3} M DPA and 0.1 M TBAP.

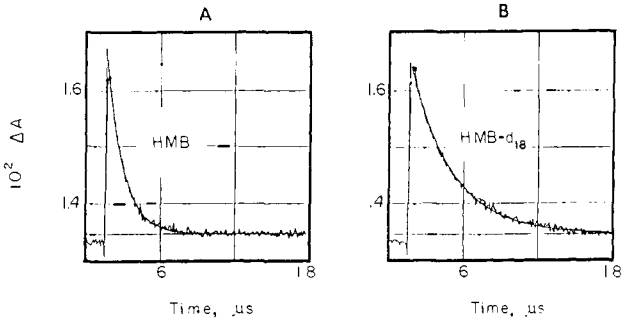

Figure 7. First-order decay of the $HMB^{\bullet+}$ absorbance at 495 nm following the CT excitation of 0.05 M HMB (left) or HMB-d_{18} (right) and 0.1 M TNM in acetonitrile containing 0.015 M lutidine and 0.1 M $LiClO_4$ at 25 °C.

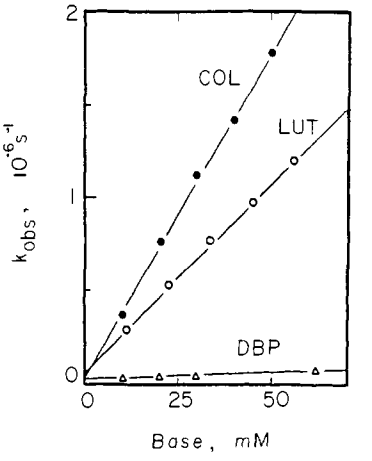

Figure 8. Quenching of $HMB^{\bullet+}$ by pyridine bases, showing the dependence of the pseudo-first-order rate constant k_{obs} from the 532-nm excitation of 0.05 M HMB and 0.1 M TNM in acetonitrile containing 0.1 M $LiClO_4$ and COL (●), LUT (○), and DBP (△).

The second-order rate constants k_{et} for the quenching of the various methylarene cation radicals by diphenylanthracene are listed in Table III. The second-order rate constants k_{-et} obtained from the appearance of $DPA^{\bullet+}$ are also included as a comparative corroboration of the kinetics.[33] The coincident values of $k_{et} = -k_{-et}$ observed under these conditions thus provided the final experimental verification of the spectral assignment of transient absorption band C to the methylarene cation radicals. Furthermore the absence of side-chain nitration (despite the CT activation of the methylarene EDA complex) indicated that the electron-transfer quenching of $ArCH_3^{\bullet+}$ in eq 16 superseded the proton transfer in eq 15, even at low levels of the electron donor.[34] It is noteworthy that the rate constants for electron transfer in Table III were rather invariant at $k_{et} = 7 \times 10^9$ M^{-1} s^{-1} and essentially that for diffusive combination ($k_{diff} = 10^{10}$ M^{-1} s^{-1}).[35] Indeed the driving forces $-\Delta G_{et}$ evaluated in Table III[36] were all sufficiently exergonic to predict a diffusion-controlled electron transfer to $ArCH_3^{\bullet+}$ from the anthracene donor DPA. The insensitivity of this exergonic electron transfer to steric effects in the highly encumbered dineopentyltetramethylbenzene (NTB) also accorded with the outer-sphere mechanism.[37]

(33) The subsequent fate of the cation radical $DPA^{\bullet+}$ formed secondarily in eq 16 was the same as that previously described in the direct CT activation of the diphenylanthracene EDA complex.[16]

(34) Note that the >50-fold higher concentrations of $ArCH_3$ relative to 9,10-diphenylanthracene in Table III ensured that irradiation at $\lambda > 425$ nm excited only the methylarene EDA complex.

(35) See: (a) Masnovi, J. M.; Kochi, J. K. in ref 17 and (b) Gordon, A. J.; Ford, R. A. *The Chemist's Companion*; Wiley: New York, 1972.

(36) Weller, A. *The Exciplex*; Gordon, M., Ware, W. R., Eds.; Academic Press: New York, 1975; Chapter 2, pp 23–28. Note that C in eq 6 is neglected here.

(37) Fukuzumi, S.; Wong, C. L.; Kochi, J. K. *J. Am. Chem. Soc.* **1980**, *102*, 2928.

Table IV. Deprotonation of Methylarene Cation Radicals by Added Bases[a]

methylarene	k_H, 10^{-7} M^{-1} s^{-1} [b]			
	LUT	COL	DBP	TBAT[c]
HMB	2.1	3.5[d]	<0.1	~0.1
HMB-d_{18}	0.75			
HEB	0.06	0.08		
PMB	4	5.4	<0.1	~0.2
DUR	5.8	8	<0.1	~0.2

[a] In 0.05 M $ArCH_3$, 0.1 M TNM, and 0.1 M $LiClO_4$ in acetonitrile containing excess base. [b] Determined under pseudo-first-order conditions at 22 °C. Average standard deviation, ±30%. [c] Tetra-*n*-butylammonium trinitromethide. [d] $k_H = 4.8 \times 10^7$ without added $LiClO_4$.

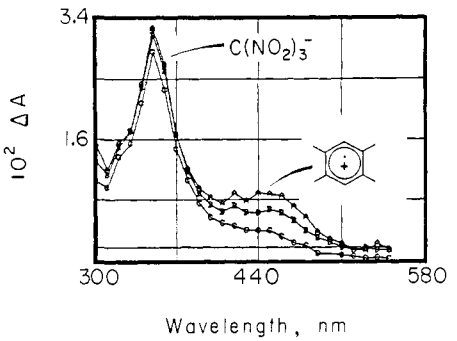

Figure 9. Time-resolved absorption spectra showing $DUR^{\bullet+}$ and $C(NO_2)_3^-$ at (top to bottom) 2, 8, and 67 μs following the 355-nm excitation of 0.1 M DUR and 0.01 M TNM in acetonitrile containing 1×10^{-3} M COL and 0.1 M $LiClO_4$.

B. Quenching of $ArCH_3^{\bullet+}$ by pyridines effectively occurred in the concentration range of 5×10^{-4} to 5×10^{-2} M lutidine. Figure 7 typically illustrates the complete return of the $HMB^{\bullet+}$ absorbance to the base line, with the excellent fit of the smooth, computed curve to the experimental decay with first-order kinetics. The linear dependence of the observed first-order rate constant on the concentration of the various pyridine bases (Figure 8) yielded the second-order rate constant k_H for the quenching of $ArCH_3^{\bullet+}$ by deprotonation, i.e.

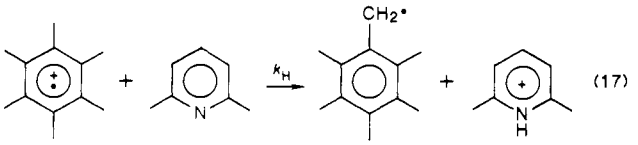

(17)

Indeed the deuterium kinetic isotope effect of $k_H/k_D = 2.8$ obtained from the comparison of k_H for HMB with that of HMB-d_{18} (Table IV) confirmed the proton transfer in eq 17.

Similar pseudo-first-order kinetics behavior was observed with the other pyridine bases, and the calculated second-order rate constants k_H are listed in Table IV, together with those obtained from various methylarene cation radicals.

The time-resolved spectra obtained from the CT activation of the durene EDA complex in the presence of added collidine (COL) were related to the competition between nuclear and side-chain nitration in eq 11 and 12, respectively. The series of time-resolved spectra in Figure 9 show that only $DUR^{\bullet+}$ underwent an accelerated decay, whereas the concentration of the trinitromethide anion was rather invariant. These kinetic results are thus completely consistent with the effect of pyridine bases on the competitive products of side-chain and nuclear nitration in eq 11 and 12 (see Figure 3).

VII. Kinetic Isotope Effects in Side-Chain CT Nitration. The kinetic acidity (k_H) and the kinetic isotope effect (k_H/k_D) in Table IV relate to the rate-limiting proton transfer from methylarene cation radicals to various added bases (see eq 17). In order to ascertain the importance of such direct deprotonations in side-chain nitration, we examined the kinetics behavior of $HMB^{\bullet+}$ in the absence of added bases, i.e., under the reaction conditions for the charge-transfer nitration outlined in Table I.[38]

Table V. Kinetic Isotope Effect in the Decay of $HMB^{\bullet+}$ in Various Solvents[a]

solvent	ϵ[b]	k_2, 10^{-5} A^{-1} s^{-1} [c]		k_H/k_D
		HMB	HMB-d_{18}	
dichloromethane	9.08	43	15	2.8
acetone	20.7	3.2	2.2	1.4
nitromethane	35.8	4.3	3.9	1.1
acetonitrile	37.5	5.1	5.0	1.0
CH_2Cl_2/MeCN (19:1)	10	17	7.5	2.2
CH_2Cl_2/MeCN (9:1)	12	8.5	5.4	1.6
CH_2Cl_2/MeCN (4:1)	16	5.3	3.7	1.4
CH_2Cl_2/MeCN (1:1)	23	6.4	6.5	1.0
		k_H, 10^{-5} s^{-1}		
solvent	ϵ[b]	HMB	HMB-d_{18}	k_H/k_D
n-hexane	1.89	27	15	1.8
benzene	2.28	33	17	2.0
diethyl ether	4.34	44	20	2.2
tetrahydrofuran	7.58	19	8.7	2.2
ethanol	24.5[d]	9.3	2.1	4.4

[a] From the CT excitation at 532 nm of 0.05 M HMB (HMB-d_{18}) and 0.1 M TNM with a 10-ns laser pulse, unless indicated otherwise. [b] Dielectric constant. [c] A = absorbance units, estimated uncertainty ± 20%. [d] 0.025 M HMB and 0.05 M TNM.

The decay profile for $HMB^{\bullet+}$ following the 532-nm excitation of the hexamethylbenzene EDA complex in acetonitrile solution with a 10-ns laser pulse showed second-order kinetics behavior[23] similar to that observed in dichloromethane (see Figure 5). However the magnitude of the second-order rate constant of $k_H = 5.1 \times 10^5$ A^{-1} s^{-1} was about 1 order of magnitude slower than that observed in the less polar solvent (vide supra). More importantly, the striking falloff in the kinetic isotope effect of $k_H/k_D = 2.8$ in dichloromethane to $k_H/k_D = 1.0$ in acetonitrile followed a monotonic trend in the various CH_2Cl_2/MeCN mixtures listed in Table V. The strong dependency of the kinetic isotope effect on the dielectric constant[39] was indicated by the intermediate values of k_H/k_D found in acetone and nitromethane. Similarly, the kinetic isotope effect observed in dichloromethane dropped off smoothly to $k_H/k_D = 1.0$ as the concentration of the added innocuous salt (tetra-*n*-butylammonium perchlorate, TBAP) was gradually increased to 0.2 M (see the Experimental Section).

In highly nonpolar solvents such as hexane and benzene, the decay profile of $HMB^{\bullet+}$ differed substantially from that observed above, and the kinetics analysis established first-order behavior. Indeed the same kinetics were observed in the ethereal solvents ether and THF. Moreover, first-order kinetics were observed in the protic solvent ethanol, despite its substantial dielectric constant.

Discussion

The viability of the electron-transfer mechanism for the nitration of methylarenes, as presented in Scheme II, is critically dependent on the behavior of the ion radical pair $[ArCH_3^{\bullet+},NO_2]$, insofar as it leads to side-chain and nuclear substitution. However, the concentration of this transitory intermediate is too low to be observed in an adiabatic process, since the activation step leading to the ion–radical pair is rate-limiting (eq 3a) and the rate constant for annihilation of $ArCH_3^{\bullet+}$ will always be faster than that for its production. As such the vertical, nonadiabatic processes effected by actinic irradiation must provide the requisite means for the alternative generation of $ArCH_3^{\bullet+}$ in sufficient concentrations for direct examination as follows.

I. Production of Ion–Radical Pairs $[ArCH_3^{\bullet+},NO_2]$ by Charge-Transfer Activation of Methylarene EDA Complexes. Mixing each of the methylarenes of Table I with tetranitromethane leads immediately to colored solutions of the electron donor–ac-

(38) The measurement of the kinetic isotope effect for side-chain nitration is practicable only with HMB owing to the substantial incursion of nuclear nitration in the other methylarenes (see Table I) that lead to large statistical dilutions of the experimental values of k_H/k_D.

(39) Dean, J. A., Ed.; *Lange's Handbook of Chemistry*, 13th ed.; McGraw-Hill: New York, 1985; p 10–103 ff.

ceptor or EDA complex (eq 6). The time-resolved spectroscopy defines the relevant photophysical and photochemical processes associated with the charge-transfer excitation of such a methylarene complex (eq 13) to form the pertinent ion radicals.[16] Accordingly the overall process can be summarized as

Scheme IV

$$ArMe + C(NO_2)_4 \overset{K}{\rightleftharpoons} [ArMe,C(NO_2)_4] \quad (18)$$

$$[ArMe,C(NO_2)_4] \xrightarrow{h\nu_{CT}} [ArMe^{\bullet+},C(NO_2)_4^{\bullet-}] \quad (19)$$

$$[ArMe^{\bullet+},C(NO_2)_4^{\bullet-}] \xrightarrow{fast} \underset{II}{[ArMe^{\bullet+},NO_2^{\bullet},C(NO_2)_3^-]} \quad (20)$$

All the experimental observations with methylarenes and tetranitromethane indeed coincide with the formulation in Scheme IV. Thus the exposure of ArMe to a nitrating agent such as TNM as in Figure 1B spontaneously affords the EDA complex in eq 18. These binary complexes are present in low steady-state concentrations owing to the limited magnitudes of K as measured by the Benesi–Hildebrand method.[40] Activation of such an EDA complex by the specific irradiation of the charge-transfer band results in a photoinduced electron transfer (eq 19) in accord with Mulliken theory.[19] The irreversible fragmentation following the electron attachement to $C(NO_2)_4$ leads to the ion–radical triad II in eq 20 (see Figure 4). The measured quantum yield of $\Phi \cong 0.1$ compares with that ($\Phi \cong 0.7$) previously obtained for anthracene.[16] Such relatively high quantum yields relate directly to the efficiency of cation–radical production in eq 20 relative to energy wastage by back-electron transfer of eq 19. Moreover the short lifetime (<3 ps) of $C(NO_2)_4^{\bullet-}$ ensures that $ArMe^{\bullet+}$,$C(NO_2)_3^-$ and $NO_2^{\bullet}$ are born as an intimate ion–radical triad II, initially trapped within the solvent cage, since this time scale obviates any competition from diffusional processes.[16,41] Let us now focus on the pathway by which the methylarene cation radical is quenched in the presence of added pyridine.

II. Direct Observation of the Kinetic Acidities of Methylarene Cation Radicals. The time-resolved spectra of transient methylarene cation radicals, coupled with the examination of the fast kinetics allowed by the use of laser-flash techniques, establish the efficient quenching of $ArCH_3^{\bullet+}$ in the presence of added pyridine bases, B. Since the values of the second-order rate constants k_H in Table IV relate to side-chain deprotonation of the methylarene cation radical (eq 17), the resultant production of the benzylic radicals $ArCH_2^{\bullet}$ provides the most direct pathway for side-chain nitration to occur, i.e.

Scheme V

$$ArCH_3^{\bullet+} + B \xrightarrow{k_H} ArCH_2^{\bullet} + BH^+ \quad (21)$$

$$ArCH_2^{\bullet} + NO_2 \xrightarrow{fast} ArCH_2NO_2 \quad (22)$$

According to Scheme V, the aromatic products derive from a rapid, subsequent reaction of $ArCH_2^{\bullet}$ with NO_2 (eq 22), which represents a facile homolytic coupling with little or no activation energy.[42]

In a more general context, proton transfer from the methylarene cation radical in eq 21 is also possible with a variety of Brønsted bases. Therefore we inquire into the structural factors that affect the deprotonation rate. Among the pyridine bases, the second-order rate constants k_H in Table IV consistently decrease in the following order: 2,4,6-collidine > 2,6-lutidine >> 2,6-di-*tert*-butylpyridine for all the methylarene cation radicals.[43] That COL is a slightly better quencher than LUT follows from a base strength that is 1.2 pK units greater.[45] Similarly, the less efficient quenching of $ArCH_3^{\bullet+}$ by the hindered base 2,6-di-*tert*-butylpyridine (DBP) can be attributed to its weaker base strength by 3.6 pK units.[46] Moreover, the similar quenching efficiencies of DBP and trinitromethide anion outlined in Table IV are more or less in line with their comparable base strengths.[47] These results taken together with the kinetic isotope effect, $k_H/k_D = 2.8$ for $HMB^{\bullet+}$, support the earlier conclusion of an early transition state for the exergonic proton transfer in eq 21 which has not proceeded beyong the symmetrical situation.[44] Such a qualitative description of methylarene cation radicals as effective Brønsted acids also accounts for the relatively low sensitivity of the second-order rate constant k_H to steric effects in the pyridine base.

Most importantly, it must be emphasized that these spectral observations of $ArCH_3^{\bullet+}$ and their unambiguous decay kinetics establish the efficacy with which pyridine bases are able to pluck methyl protons from $ArCH_3^{\bullet+}$ on its pathway to side-chain nitration, as summarized in Scheme V. Let us now direct our attention to how these deprotonations pertain to the charge-transfer nitration of methylarenes in the absence of extra pyridine bases.

III. Mechanism of Charge-Transfer Nitration of Methylarene EDA Complexes. The excellent material balance obtained in charge-transfer nitration (Table I) demands that the ion–radical triad II in Scheme IV proceeds quantitatively to the side chain nitration products according to the stoichiometry

$$\underset{II}{[ArCH_3^{\bullet+},NO_2,C(NO_2)_3^-]} \rightarrow ArCH_2NO_2 + HC(NO_2)_3 \quad (23)$$

Such a transformation of the triad II can be readily accommodated from the deprotonation results in Scheme V by a succession of bimolecular steps, viz.

Scheme VI

$$ArCH_3^{\bullet+} + C(NO_2)_3^- \xrightarrow{k_H} ArCH_2^{\bullet} + HC(NO_2)_3 \quad (24)$$

$$ArCH_2^{\bullet} + NO_2 \xrightarrow{fast} ArCH_2NO_2 \quad (22)$$

According to Scheme VI, the role of base in CT nitration is now relegated to the trinitromethide anion. Indeed the sizeable value of $k_H = 1 \times 10^6$ M^{-1} s^{-1} was independently evaluated for eq 24 in Table IV from the pseudo-first-order kinetics for the quenching of $HMB^{\bullet+}$ by the extra presence of *added* trinitromethide salt n-$Bu_4N^+C(NO_2)_3^-$. Further support for Scheme VI also derives from the kinetic isotope effect observed directly from HMB and HMB-d_{18} during charge-transfer nitration in dichloromethane (see Table V).[48] Thus the value of $k_H/k_D = 2.8$ for the second-order decay of $HMB^{\bullet+}$ in Figure 5 is identical with that obtained from the pseudo-first-order quenching of $HMB^{\bullet+}$ by added pyridine in eq 17.[49]

The rather straightforward explanation for side-chain substitution in Scheme VI however cannot represent the generalized mechanism for charge-transfer nitration, since it is inconsistent with the singular absence of the kinetic isotope effect obtained in acetonitrile and nitromethane (Table V). Accordingly, we are forced to conclude that the direct deprotonation of $HMB^{\bullet+}$ (as

(40) Benesi, H. A.; Hildebrand, J. H. *J. Am. Chem. Soc.* **1949**, *71*, 2703. (b) Person, W. B. *J. Am. Chem. Soc.* **1965**, *87*, 167.

(41) Chaudhuri, S. A.; Asmus, K. D. *J. Phys. Chem.* **1972**, *76*, 26.

(42) Compare: Giamalva, D. H.; Kenion, G. B.; Church, D. F.; Pryor, W. A. *J. Am. Chem. Soc.* **1987**, *109*, 7059.

(43) Where there is overlap, the values of k_H in Table IV are equivalent to k_2 evaluated earlier in ref 44, if cognizance is taken of the uncertainty of ΔE in eq 21 of the previous study. Accordingly, we propose the slightly revised values of $E°$ = 1.72, 1.80, and 1.87 V vs SCE for HMB, PMB, and DUR, respectively, in acetonitrile.

(44) Schlesener, C. J.; Amatore, C.; Kochi, J. K. *J. Am. Chem. Soc.* **1984**, *106*, 7472.

(45) (a) Cauquis, G.; Deronzier, A.; Serre, D.; Vieil, E. *J. Electroanal. Chem.* **1975**, *60*, 205. (b) See also: Perrin, D. D.; Dempsey, B.; Serjeant, E. P. *pK_a Prediction from Organic Acids and Bases*; Chapman and Hall: London, 1981.

(46) Benoit, R. L.; Frêchette, M.; Lefebvre, D. *Can. J. Chem.* **1988**, *66*, 1159.

(47) Hall, T. N. *J. Org. Chem.* **1964**, *29*, 3587. Pearson, R. G.; Dillon, R. L. *J. Am. Chem. Soc.* **1953**, *75*, 2439.

(48) Thus the base strength of $C(NO_2)_3^-$, that is no less than 5 pK units of lutidine, predicts a kinetic isotope effect $k_H/k_D \leq 5$ for proton transfer in eq 24.[44]

(49) For similar values of k_H/k_D determined under other circumstances, compare: (a) Parker, V. D.; Tilset, M. *J. Am. Chem. Soc.* **1986**, *108*, 6371. (b) Schlesener, C. J.; Amatore, C.; Kochi, J. K. *J. Am. Chem. Soc.* **1984**, *106*, 3567.

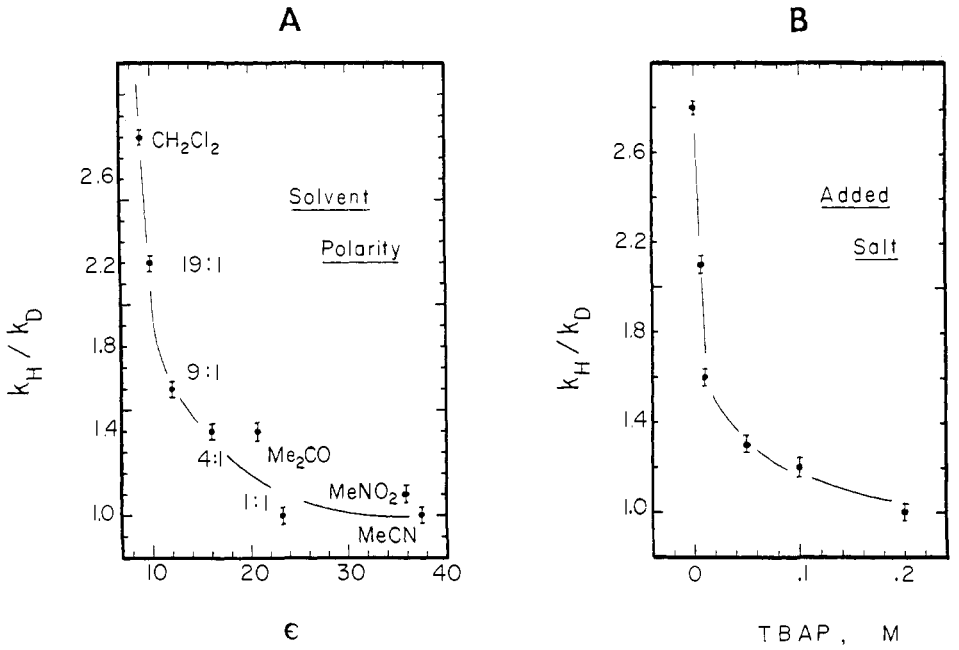

Figure 10. The kinetic isotope effect (k_H/k_D) in the charge-transfer nitration of HMB and HMB-d_{18} as a function (left) of the bulk dielectric of the solvent (ratios are CH_2Cl_2:MeCN) and (right) of added TBAP in dichloromethane.

in Scheme VI) does not materially contribute to the charge-transfer nitration of hexamethylbenzene in the more polar solvents. Let us therefore consider the alternative sequence of bimolecular steps for the annihilation of the ion–radical triad II formed in eq 20 (Scheme IV), viz.

Scheme VII

$$ArCH_3^{\bullet+} + NO_2^{\bullet} \xrightarrow{k_c} ArCH_3(NO_2)^+ \quad (25)$$

$$ArCH_3(NO_2)^+ + C(NO_2)_3^- \rightarrow ArCH_2NO_2 + HC(NO_2)_3 \quad (26)$$

According to Scheme VII, the annihilation of the ion-radical pair in eq 25 to form the cationic adduct is rate-limiting. Since such an ipso addition is akin to the formation of the Wheland intermediate,[50] the rate of the subsequent deprotonation in eq 26 is expected to be rapid and to show no or little kinetic isotope effect.[51]

Schemes VI and VII present an interesting mechanistic conundrum since they only differ in the sequence by which the pairwise interactions of the triad II occurs. We note however that side-chain nitration according to Scheme VI is fundamentally distinguished from that in Scheme VII by the ion–radical dynamics of the activation step. In other words, Scheme VI represents the initial, rate-limiting collapse of the metastable triad II as the *ion pair*, whereas Scheme VII first involves the fragments as the *radical pair*. Fortunately this dichotomy was resolved in an earlier study,[53] by taking cognizance of the overwhelming differences in coulombic energy between ion-pair and radical-pair annihilations, as described in eq 24 and 25, respectively. In particular the application of solvent polarity and salt effects can be used to modulate the electrostatic interactions in two ways. (i) the cationic $ArCH_3^{\bullet+}$ and anionic $C(NO_2)_3^-$ initially formed as the contact ion pair in Scheme IV are effectively dissociated as separate ions by polar solvents with relatively high dielectric constants,[17,54] e.g.

$$ArCH_3^{\bullet+},C(NO_2)_3^- \underset{}{\overset{MeCN}{\rightleftharpoons}} ArCH_3^{\bullet+} + C(NO_2)_3^- \quad (27)$$

(ii) Ion-pair exchange with innocuous salts such as lithium perchlorate serves to isolate the reactive partners, e.g.[17,54]

$$ArCH_3^{\bullet+},C(NO_2)_3^- + Li^+ClO_4^- \rightleftharpoons ArCH_3^{\bullet+},ClO_4^- + Li^+C(NO_2)_3^- \quad (28)$$

As applied to the ion–radical triad II, polar solvents such as acetonitrile will stabilize the solvent-separated ion pair and thus present an optimum opportunity for the alternative, homolytic coupling in eq 25 (Scheme VII) to take place by default.[55] In other words, the rate-limiting deprotonation (Scheme VI) and homolytic coupling (Scheme VII) represent competing processes, the continuous variation between which is modulated by solvent variation as it affects ion-pair separation.[54] Indeed Figure 10A confirms this analysis by utilizing the kinetic isotope effect (k_H/k_D) and the dielectric constant (ϵ) as experimental measures of the competitive mechanisms as a function of the interionic separations in eq 27. The inclusion of all the data obtained from widely varying mixtures of the extreme solvents (CH_2Cl_2 and MeCN) in the smooth correlation indicates the sensitivity of k_H/k_D to lie with the bulk dielectric of the medium and not with the specific solvation of the ions. The validity of this formulation is also reinforced in Figure 10B by the continuous variation of k_H/k_D with the added innocuous salt (TBAP) in the less polar solvent dichloromethane. Importantly, the sharp drop-off of k_H/k_D at low concentrations (<0.01 M) of added salt is strongly reminiscent of the kinetics behavior of contact (intimate) ion pairs—with the exchange in eq 28 designated as the "special" salt effect by

(50) Ingold, C. K. *Structure and Mechanism in Organic Chemistry*, 2nd ed.; Cornell University Press: Ithaca, New York, 1969; pp 331 ff.

(51) (a) Similar to the Wheland intermediate, the β-deprotonation of the cationic ipso adduct (eq 2b) is facile[8] and expected to show no deuterium isotope effect.[52] (b) The subsequent rearrangement of the resultant methylenenitrocyclohexadiene (MC) to the side chain substitution product is intramolecular (S_Ni'). (See: Fischer, A.; Ramsay, J. N. *Can. J. Chem.* **1974**, *52*, 3960; *J. Am. Chem. Soc.* **1974**, *96*, 1614.) (c) It has also been proposed that products of side-chain substitution arise via an intermolecular S_N2' substitution of MC by different nucleophiles.[66] (d) According to Scheme VII, the observed second-order kinetics in acetonitrile (Figure 5) relate to the rate of the radical-pair collapse in eq 25. Trinitromethide is involved in the fast step (eq 26 via MC) subsequent to this rate-limiting process. A similar kinetics situation was described for nuclear nitration in ref 25 and 53. (e) It is also possible for MC to react by other pathways, such as loss of a cationic methyl moiety. However these are minor owing to the excellent material balance obtained in the CT nitration of hexamethylbenzene in acetonitrile. (f) The side-chain nitrates presumably arise from the further oxidation of the corresponding nitrites,[80] but the role of additives is unclear.

(52) Melander, L. *Ark. Kemi* **1950**, *2*, 211. Halvarson, K.; Melander, L. *Ark. Kemi* **1957**, *11*, 77. See also: Melander, L. *Isotope Effects on Reaction Rates*; Ronald Press: New York, 1960.

(53) Sankararaman, S.; Haney, W. A.; Kochi, J. K. *J. Am. Chem. Soc.* **1987**, *109*, 7824.

(54) Bockman, T. M.; Kochi, J. K. *J. Am. Chem. Soc.* **1988**, *110*, 1294.

(55) Owing to the conservation of charge in eq 25, the rate constant k_c is considered to be solvent insensitive. For a similar kinetics situation in aromatic nitration, see Sankararaman et al. in ref 53.

Winstein and co-workers in their pioneering studies of the solvolysis mechanism in aliphatic nucleophilic substitution.[56,57]

Thus the direct observation of $HMB^{\bullet+}$ coupled with the measurement of the kinetic isotopic effects compel us to a composite mechanism for charge-transfer nitration. It is particularly noteworthy that the competing pathways in Schemes VI and VII, despite their apparent differences, are kinetically quite akin since only minor changes in solvent polarity and salt concentrations are sufficient to alter the balance from ion-pair (eq 24) to radical-pair (eq 25) interactions. At one extreme of high solvent polarity (acetonitrile) the decay kinetics for $HMB^{\bullet+}$ (Table V) yield the rate-limiting homolytic coupling in eq 25 with the second-order rate constant of $k_c = 5 \times 10^5\ A^{-1}\ s^{-1}$. Contrastingly, in the less polar solvent dichloromethane, the decay kinetics for $HMB^{\bullet+}$ in Figure 5 depicts the rate-limiting proton transfer in eq 24 with the second-order rate constant of $k_H = 4 \times 10^6\ A^{-1}\ s^{-1}$. The comparable magnitudes of k_c and k_H generally set the lifetime of $HMB^{\bullet+}$ in charge-transfer nitration to ~200 ns. The latter represents the lifetime of the contact ion pair in highly nonpolar solvents such as *n*-hexane, benzene, and diethyl ether, in which the ion-pair separation is disfavored[53] and the first-order rate constant occurs with $k_1 \cong 3 \times 10^6\ s^{-1}$ (Table V).[58]

Since the lifetimes of $ArCH_3^{\bullet+}$ as carbon acids are limited by their kinetic acidities, the presence of added pyridine will also tilt the competition from homolytic coupling in (Scheme VII) to deprotonation (Scheme V, B = py). Such a change in mechanism is manifested in the charge-transfer nitration of durene by a change in the product composition described by eq 11 and 12. The competition is illustrated in Figure 3, which represents the obliteration of nuclear nitration in favor of side-chain substitution by the increased rate of deprotonation of $DUR^{\bullet+}$ in the presence of added base according to eq 21. When all of the cation radical $DUR^{\bullet+}$ is quenched by the added base, the trimethylbenzyl radical is the sole source of the aromatic products.[60]

In the absence of an added pyridine base, the charge-transfer nitration of durene in acetonitrile occurs principally via radical-pair collapse of the triad II.[61] Accordingly, the 3:1 ratio of side-chain/nuclear nitration of durene in Table I largely reflects the collapse at either an ipso or unsubstituted nuclear position, i.e.[62]

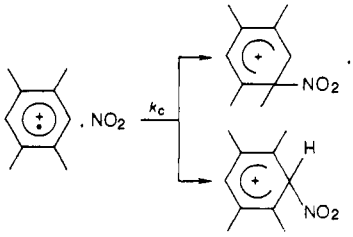

. etc. (29)

(30)

The alternative ion-pair interaction of the triad II from durene will be promoted by less polar solvents such as dichloromethane (see Figure 10A)—with two important consequences. First, the side-chain nitration is partially replaced by side-chain trinitromethylation, and nuclear trinitromethylation is now observed (Table II, entry 10). Nuclear trinitromethylation clearly derives from ion-pair collapse at the unsubstituted position.[63] As such,

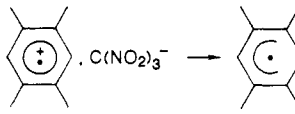

. etc. (31)

it is not an important process in the more polar acetonitrile (Table I). Indeed the solvent effect on such a nuclear substitution is unambiguously manifested in the case of mesitylene, which affords 50% yields of (trinitromethyl)mesitylene in dichloromethane (Table II, entry 12) but <5% in acetonitrile (Table I).

The side-chain trinitromethylation of durene most likely arises from the neutralization of trinitromethide anion by the trimethylbenzyl cation that is readily formed by the facile oxidation of the radical.[64] However the relatively large amounts of side-chain trinitromethylation of hexamethylbenzene obtained even in acetonitrile (Table I) suggest that the ipso adduct in Scheme VII also may be an intermediate.[51,65]

IV. Comments on the Mechanism of the Thermal (Adiabatic) Nitration of Methylarenes. The mechanistic delineation of charge-transfer nitration according to Schemes VI and VII provides further insight into side-chain nitrations that are conventionally carried out thermally with nitric acid.[4] For example, Table VI lists the aromatic products derived from the nitric acid treatment of the same methylarenes that are examined in this study.[5,66] Indeed the ratios of ipso/nuclear attack in column 4 (Table VI)[67] bear a striking relationship with the relative side-chain/nuclear substitutions that are given in Table I. Such a parallel trend, despite the wide variations in the (attack) product ratios, is not fortuitous but indicates a strong similarity of reactive intermediates in charge-transfer and thermal nitration. Let us therefore examine the interrelationship in two parts, by first focusing on the mechanism of side-chain nitration and then relating it to the competition between side-chain and nuclear nitration as follows.

Charge-transfer nitration of methylarenes demonstrates the viability of the cation radicals $ArCH_3^{\bullet+}$ as intermediates in dual mechanisms for side-chain substitution. The competition between the pathways in Schemes VI and VII (modulated by the solvent

Table VI. Nitration of Methylarenes with Nitric Acid[a]

methylarene	% $ArNO_2$[b]	% $ArCH_2NO_2$[c]	ipso/nucl[i]
MES	100	0	0/100
DUR	85[d]	15[e]	75/25
PMB	55	45[f]	82/18
HMB[g]		100[h]	100/0

[a] With HNO_3 in acetic anhydride at 0 °C, unless indicated otherwise (from ref 5). [b] Ring nitration product. [c] Side chain nitration product. [d] Includes 33% acetate. [e] Includes 3% aldehyde and 6% alcohol. [f] Includes 8% aldehyde. [g] With HNO_3 in acetic acid at 15 °C (from ref 66). [h] Includes 44% nitrate and alcohol and 30% acetate. [i] Ratio of attack at ipso/unsubstituted nuclear positions (from ref 67).

(56) (a) Winstein, S.; Klinedinst, P. E., Jr.; Robinson, G. C. *J. Am. Chem. Soc.* **1961**, *83*, 885. (b) Winstein, S.; Klinedinst, P. E., Jr.; Clippinger, E. *J. Am. Chem. Soc.* **1961**, *83*, 4986. (c) Winstein, S.; Robinson, G. C. *J. Am. Chem. Soc.* **1958**, *80*, 169 and related papers.

(57) For reviews, see: (a) Harris, J. M. *Prog. Phys. Org. Chem.* **1974**, *11*, 89. (b) Szwarc, M., Ed.; *Ions and Ion Pairs in Organic Reactions*; Wiley-Interscience: New York, 1974; Vol. 2, Chapter 3, p 247 ff.

(58) (a) The equilibrium in eq 27 to yield kinetically free ions is considered to be minimal in these highly nonpolar solvents. As such, first-order kinetics prevail for ion-pair interactions like those in eq 24. (b) In highly nonpolar solvents, the intrusion of ion-pair aggregates[59] presents a number of complicating factors in the kinetics interpretation, such as the variation of k_H/k_D in Table V (entries 9–12), the competition in ambident selectivity, and radical-pair collapse.

(59) Compare: Goodson, B. E.; Schuster, G. B. *J. Am. Chem. Soc.* **1984**, *106*, 7254; *Tetrahedron Lett.* **1986**, *27*, 3123.

(60) For the quantitative analysis of durene products in the presence of added lutidine, see the Experimental Section.

(61) This conclusion is also supported by the value of k_H for lutidine which is 30-fold greater than that for trinitromethide (Table IV), together with the somewhat limited slope in Figure 8.

(62) Based on negligible reversibility.

(63) (a) Ipso collapse in eq 31 is disfavored by the severe steric crowding at the tertiary center. (b) The subsequent step leading to nuclear trinitromethylation from the intermediate in eq 31 will be rapid (see ref 25 and 53).

(64) See: (a) Rollick, K.; Kochi, J. K. *J. Am. Chem. Soc.* **1982**, *104*, 1319. (b) Khudyakov, I. V.; Kuz'min, V. A. *Russ. Chem. Rev.* (*Engl. Transl.*) **1978**, *47*, 22. Oxidation of α-substituted alkyl radicals by TNM occurs at diffusion-controlled rates. See: (c) Göbl, M.; Asmus, K.-D. *J. Chem. Soc., Perkin Trans. 2* **1984**, 691. (d) Eibenberger, J.; Schulte-Frohlinde, D.; Steenken, S. *J. Phys. Chem.* **1980**, *84*, 704. (e) For redox properties of related radicals, see: Wayner, D. D. M.; McPhee, D. J.; Griller, D. *J. Am. Chem. Soc.* **1988**, *110*, 132.

(65) Hydrogen atom abstraction from the radical cation also would lead to a benzylic cation. Nitrogen dioxide can react by allylic hydrogen abstraction: Pryor, W. A.; Lightsey, J. W.; Church, D. F. *J. Am. Chem. Soc.* **1982**, *104*, 6685. Titov, A. I. *Tetrahedron* **1963**, *19*, 557.

(66) Suzuki, H.; Mishina, T.; Hanafusa, T. *Bull. Chem. Soc. Jpn.* **1979**, *52*, 191.

(67) Fischer, A.; Wright, G. J. *Aust. J. Chem.* **1974**, *27*, 217.

polarity and added salts) is clearly delineated by the kinetic isotope effect ($k_H/k_D \sim 3$) for the deprotonation of $HMB^{\bullet+}$ by Brønsted base such as lutidine or trinitromethide anion. If a similar deprotonation of $HMB^{\bullet+}$ were to pertain to the thermal nitration, as initially depicted in Scheme II, a substantial kinetic isotope effect is expected.[48] Thus the observation that the side-chain nitration of hexamethylbenzene with nitric acid occurs with no kinetic isotope effect[66] militates against Scheme II. Accordingly, the alternative pathway involving the initial radical-pair annihilation analogous to that presented in Scheme VII could account for the absence of a kinetic isotope effect, i.e.

Scheme VIII

$$ArCH_3 + NO_2^+ \rightarrow ArCH_3^{\bullet+} + NO_2 \quad (32)$$

$$ArCH_3^{\bullet+} + NO_2 \rightarrow ArCH_3(NO_2)^+ \quad (33)$$

$$ArCH_3(NO_2)^+ \xrightarrow[-H^+]{\text{fast}} ArCH_2NO_2 \quad (34)$$

Such a mechanism for side-chain nitration involves the same cationic ipso adduct as that presented in Scheme I.

According to the formulation in Scheme VIII, the competition between side-chain and nuclear nitration of durene (eq 1) arises during the radical-pair collapse of $DUR^{\bullet+}$ at either an ipso or an unsubstituted nuclear position (see eq 29 and 30). Since both homolytic couplings are facile ($k_c \cong 10^6$ A^{-1} s^{-1}), the expected small differences in activation energies should be reflected in the spin densities of $ArCH_3^{\bullet+}$ at the ipso and unsubstituted positions. Electronic effects, steric effects, and reversibility as factors effecting the selectivity in such an ion–radical collapse have been recently delineated and require no further elaboration.[68] Suffice it to emphasize here that the ipso adduct and Wheland σ-complex in eq 29 and 30 determine the competition between side-chain and nuclear nitration insofar as the follow-up deprotonations are rapid and irreversible. These adducts are reactive intermediates that are common to both charge-transfer (Scheme VII) and thermal nitration (Scheme I). Whether the methylarene cation radical is also the common precursor in thermal nitration will depend on the adiabatic electron transfer (eq 32), which is not directly addressed by the experimental results herein.[69] Since the methylarene cation radical is the obligatory intermediate in charge-transfer nitration, the most economical formulation reconciles their similarity with an optimum number of common intermediates. Hopefully the rate-limiting electron transfer in eq 32, to be examined separately, will resolve this final question.[69]

Experimental Section

Materials. Hexamethylbenzene (Fluka), hexaethylbenzene (Eastman), pentamethylbenzene (Aldrich), and durene (Aldrich) were purified by recrystallization from ethanol. Mesitylene (Aldrich) was purified by distillation. 2,4,6-Collidine and 2,6-lutidine (Matheson, Coleman and Bell) as well as 2,6-di-*tert*-butylpyridine (Aldrich) were distilled from potassium hydroxide. Tetra-*n*-butylammonium trinitromethide[17] and tetranitromethane[16] were prepared according to literature procedures. Lithium perchlorate and tetra-*n*-butylammonium perchlorate (G. F. Smith) and tetra-*n*-butylammonium hexafluorophosphate (Aldrich) were recrystallized from a mixture of acetonitrile and ethyl acetate and dried over P_2O_5 in vacuo. Hexamethylbenzene-d_{18} (Merck Sharp and Dohme Isotopes) and 9,10-diphenylanthracene (Aldrich) were used as received. Acetonitrile (Fisher HPLC grade) and dichloromethane (Fisher) were distilled from P_2O_5 and stored under an argon atmosphere. Hexane (Baker) was distilled from sodium under an argon atmosphere. Reinecke salt was obtained from Aldrich. The products of charge-transfer nitration were synthesized independently as follows.

Pentamethylbenzyl Chloride. A mixture of pentamethylbenzene (7 g, 50 mmol), glacial acetic acid (15 mL), concentrated hydrochloric acid (30 mL), and 37% aqueous formaldehyde solution (10 g) was heated at 60–65 °C for 6 h. The solid was washed several times with water; the colorless, crystalline solid thus obtained (9.37 g, 95%) was recrystallized from a mixture of hexane and benzene at −20 °C. Pentamethylbenzyl chloride: mp 80 °C (lit.[70] mp 81–82 °C). ^1H NMR ($CDCl_3$): 4.73 (s, 2 H, CH_2), 2.35 (s, 6 H), 2.23 (s, 9 H) ppm.

Pentamethylbenzyl Alcohol. To a stirred solution of silver nitrate (0.95 g, 5.6 mmol) in acetone (30 mL) and water (20 mL) was added pentamethylbenzyl chloride (1 g, 5 mmol). The mixture was stirred at room temperature for 3 h, and the precipitated silver chloride was removed. The filtrate was extracted with ether, and the ether extract was dried over anhydrous magnesium sulfate. Removal of the ether in vacuo yielded pentamethylbenzyl alcohol as a colorless, crystalline solid in essentially quantitative yield: mp 160–162 °C (lit.[71] mp 162–163 °C). ^1H NMR ($CDCl_3$): 4.75 (s, 2 H, CH_2), 2.34 (s, 6 H), 2.23 (s, 9 H), 1.52 (s, br, OH) ppm. MS, *m/e* (70 eV): 179 (5), 178 (43, M^+), 161 (20), 160 (100), 145 (55), 119 (20), 91 (20), 77 (12).

Pentamethylbenzyl Nitrate.[72] To a stirred solution of pentamethylbenzyl chloride (1 g, 5 mmol) in acetonitrile (15 mL) was added dropwise a solution of silver nitrate (0.94 g, 5.5 mmol) in acetonitrile (15 mL). During the addition, a white precipitate formed. The mixure was stirred for 2.5 h at room temperature and then filtered. The filtrate was evaporated to dryness to yield colorless crystals of pentamethylbenzyl nitrate in quantitative yield. Pure nitrate was obtained by recrystallization from a benzene–hexane mixture at −20 °C: mp 97 °C (lit.[72] mp 95–97 °C). IR (KBr): 2998 (m), 2930 (m), 2891 (m), 1625 (s, ONO_2), 1611 (s), 1305 (s), 1280 (m, ONO_2), 960 (s), 897 (m), 873 (m), 758 (m) cm^{-1}. ^1H NMR ($CDCl_3$): 5.62 (s, 2 H, CH_2), 2.30 (s, 6 H), 2.23 (s, 9 H) ppm. ^{13}C NMR ($CDCl_3$): 137.2, 134.4, 133.1, 124.7, 71.4 (CH_2), 17.2, 16.7, 16.4 ppm.

Pentamethylbenzyl Nitrite.[73] Solid silver nitrite (0.92 g, 6 mmol) was added to a well-stirred solution of pentamethylbenzyl chloride (1 g, 5 mmol)) in acetonitrile (15 mL) under an argon atmosphere. After stirring of the mixture for 3 h at room temperature, the silver chloride precipitate was removed. The filtrate was evaporated to dryness to yield a semisolid, the ^1H NMR spectrum of which indicated the presence of two products with singlet resonances at 5.76 and 5.64 ppm that corresponded to pentamethylbenzyl nitrite and pentamethylphenylnitromethane, respectively, in a 2:1 molar ratio. Recrystallization from hexane at −20 °C yielded pentamethylbenzyl nitrite as a low-melting, colorless crystalline solid. IR (neat): 2921 (m), 1638 (s, ONO), 1593 (s), 1554 (s), 1458 (m), 1385 (m), 1366 (m), 1352 (m), 1277 (w), 961 (m), 816 (s), 776 (s) cm^{-1}. ^1H NMR ($CDCl_3$):[73] 5.76 (s, 2 H, CH_2), 2.26 (s, 6 H), 2.23 (s, 9 H) ppm. Upon standing at room temperature in air, pentamethylbenzyl nitrite slowly decomposed to pentamethylbenzyl alcohol.

2,4,5-Trimethylbenzyl Chloride. A mixture of 1,2,4-trimethylbenzene (6 g, 0.05 mmol), acetic acid (15 mL), concentrated hydrochloric acid (30 mL), and 37% aqueous formaldehyde solution (6 mL) was heated at 60–65 °C for 6 h. The mixture was cooled and extracted with ether. The combined ether extracts were washed with aqueous bicarbonate solution and dried over anhydrous magnesium sulfate. Evaporation of the solvent produced a pale yellow, viscous oil, which yielded pure 2,4,5-trimethylbenzyl chloride upon fractional distillation in vacuo. ^1H NMR ($CDCl_3$): 7.05 (s, 1 H), 6.96 (s, 1 H), 4.55 (s, 2 H, CH_2), 2.34 (s, 3 H), 2.21 (s, 6 H) ppm.

2,4,5-Trimethylbenzyl nitrate was prepared from 2,4,5-trimethylbenzyl chloride (0.85 g, 5 mmol) and silver nitrate (0.85 g, 5.2 mmol) by the same procedure described for pentamethylbenzyl nitrate. IR (neat): 2926 (s), 1628 (s, ONO_2), 1507 (m), 1458 (m), 1278 (s, ONO_2), 966 (w), 922 (w), 859 (s), 758 (m) cm^{-1}. ^1H NMR ($CDCl_3$): 7.08 (s, 1 H), 6.98 (s, 1 H), 5.39 (s, 2 H, CH_2), 2.31 (s, 3 H), 2.22 (s, 6 H) ppm.

2,4,5-Trimethylbenzyl Nitrite. Solid silver nitrite (0.8 g, 5.2 mmol) was added to a solution of 2,4,5-trimethylbenzyl chloride (0.85 g, 5 mmol) in acetonitrile (15 mL) under an argon atmosphere. The solution was stirred for 3 h, and the silver chloride precipitate was removed. Solvent removal in vacuo from the filtrate yielded a colorless, viscous oil. ^1H NMR spectrum of the crude product showed two singlet resonances at 5.70 and 5.43 ppm corresponding to the formation of 2,4,5-trimethylbenzyl nitrite and (2,4,5-trimethylphenyl)nitromethane. The latter was identified by comparing the spectra with that of an authentic sample. Attempts to isolate the nitrite by fractional crystallization were unsuccessful. Upon standing at room temperature, the nitrite slowly decomposed to give 2,4,5-trimethylbenzaldehyde and NO_2 fumes. After complete decomposition of the nitrite, the mixture contained (2,4,5-trimethylphenyl)nitromethane and 2,4,5-trimethylbenzaldehyde. The latter was identified by comparison of the GC and GC–MS with those an authentic sample.

(68) (a) Lau, W.; Kochi, J. K. *J. Am. Chem. Soc.* **1986**, *108*, 6720. (b) See also: Fukuzumi, S.; Kochi, J. K. *J. Am. Chem. Soc.* **1981**, *103*, 7240.
(69) See: Eberson, L.; Radner, F. *Acc. Chem. Res.* **1987**, *20*, 53.
(70) Bennington, F.; Morin, R. D.; Clark, L. D. *J. Org. Chem.* **1958**, *23*, 2034.
(71) Wassermann, H. H.; Mariano, P. S.; Keehn, P. M. *J. Org. Chem.* **1971**, *36*, 1765.
(72) Suzuki, H. *Bull. Chem. Soc. Jpn.* **1970**, *43*, 879.
(73) Suzuki, H. *Nippon Kagaku Kaishi* **1978**, *7*, 1049.

2-Nitromesitylene.[74] A solution of mesitylene (0.7 mL, 5 mmol) in acetic anhydride (1 mL) was added to the nitrating mixture prepared from anhydrous nitric acid (0.22 mL, 5.2 mmol) and acetic anhydride (2 mL) at 0 °C. The mixture was stirred at room temperature for 1 h and poured onto crushed ice. 2-Nitromesitylene precipitated as a pale yellow solid which was filtered, washed with ice cold water, and dried. The yield of the crude product was 0.72 g (87%). Pure 2-nitromesitylene was obtained as a colorless, crystalline solid by recrystallization from an ether–hexane mixture at −20 °C: mp 44 °C (lit.[74] mp 44 °C). ^{1}H NMR ($CDCl_3$): 6.91 (s, 2 H, aromatic), 2.31 (s, 3 H, 5-CH_3), 2.28 (s, 6 H, 1,3-CH_3) ppm. MS, *m/e* (70 eV): 166 (5), 165 (49), 120 (37), 119 (15), 118 (13), 117 (18), 115 (18), 104 (17), 103 (26), 93 (70), 92 (18), 91 (100), 79 (25), 78 (19), 77 (68), 65 (30).

Nitration of Durene in Acetic Anhydride.[74] Anhydrous nitric acid (100 μL, 2.3 mmol) was added to a stirred slurry of durene (0.27 g, 2 mmol) in acetic anhydride (5 mL) at 0 °C. Stirring was continued for 1 h at room temperature, and the reaction mixture was worked up with aqueous ammonium hydroxide and extracted with ether. The ether extract was dried over anhydrous $MgSO_4$. Removal of ether in vacuo gave a pale yellow, viscous oil. It was dissolved in hexane, and the solution kept at −20 °C afforded 3-nitrodurene as a colorless, crystalline solid: mp 111–112 °C (lit.[74] mp 112 °C). ^{1}H NMR ($CDCl_3$): 7.05 (s, 1 H, aromatic), 2.25 (s, 6 H), 2.11 (s, 6 H) ppm. MS, *m/e* (70 eV): 180 (10), 179 (100, M^+), 162 (80), 134 (73), 133 (29), 119 (20), 118 (20), 117 (49), 116 (18), 115 (42), 107 (73), 106 (15), 105 (56), 103 (15), 93 (25), 92 (15), 91 (91), 79 (40), 78 (13), 77 (56), 65 (29). The mother liquor was evaporated and left to stand at room temperature upon which colorless crystals of 2,4,5-trimethylbenzaldehyde separated. They were washed with hexane and dried in vacuo. ^{1}H NMR ($CDCl_3$): 10.2 (s, 1 H, C*H*O), 7.55 (s, 1 H), 7.03 (s, 1 H), 2.59 (s, 3 H), 2.29 (s, 6 H) ppm. MS, *m/e* (70 eV): 148 (75, M^+), 147 (100), 119 (50), 105 (17), 91 (24), 77 (17). The hexane washings were combined, concentrated, and left in the freezer at −20 °C overnight to yield (2,4,5-trimethylphenyl)nitromethane as a colorless, crystalline solid. ^{1}H NMR ($CDCl_3$): 7.08 (s, 1 H), 6.98 (s, 1 H), 5.38 (s, 2 H, CH_2), 2.29 (s, 3 H), 2.22 (s, 6 H) ppm. MS, *m/e* (70 eV): 179 (5, M^+), 134 (11), 133 (100), 105 (12), 91 (13), 77 (6).

(2,3,4,5-Tetramethylphenyl)nitromethane.[74] Pentamethylbenzene (0.3 g, 2 mmol) was nitrated in acetic anhydride as described above with durene. (2,3,4,5-Tetramethylphenyl)nitromethane was isolated as a colorless, crystalline solid from the crude product by recrystallization from an ether–hexane mixture at −20 °C: mp 51 °C (lit.[74] mp 51–52 °C). ^{1}H NMR ($CDCl_3$): 6.99 (s, 1 H), 5.45 (s, 2 H, CH_2), 2.26 (s, 6 H), 2.22 (s, 6 H), ppm. MS, *m/e* (70 eV): 193 (6, M^+), 148 (12), 147 (100), 119 (10), 117 (10), 91 (17), 77 (7), 65 (6).

Instrumentation. The electronic spectra were recorded on a Hewlett-Packard 8450A diode-array UV–vis spectrometer. NMR spectra were recorded on a JEOL FX 90Q spectrometer operating at 90 MHz for ^{1}H NMR and 22.5 MHz for ^{13}C NMR. Proton chemical shifts are reported in ppm downfield from a $(CH_3)_4Si$ internal standard. Carbon-13 chemical shifts are reported in ppm, and the center of the multiple resonance of $CDCl_3$ (δ = 77.0 ppm) was taken as reference. IR spectra were recorded on a Nicolet 10 DX FT spectrometer. Melting points were determined on a Mel-Temp (Laboratory Devices) apparatus and are uncorrected. Routine GC analyses were carried out on a Hewlett-Packard 5790A chromatograph using a 12.5 M SE-30 (cross-linked methylsilicone) capillary column. The GC–MS analyses were carried out on a Hewlett-Packard 5890 chromatograph interfaced to a HP5970 mass spectrometer (EI, 70 eV) and also on a Finnigan TSQ GC/MS/MS/DS system.

Time-Resolved Absorption Spectra and the Decay of the Spectral Transients. Time-resolved differential absorption spectra of the transient intermediates were obtained on three laser-flash systems. The 532-nm (second harmonic) or 355-nm (third harmonic) pulse from a Quantel YG 481 Nd^{3+}:YAG laser (pulse width 11 ns, Q-Switched), or a Quantel YG 581 laser (pulse width 11 ns, Q-Switched) or a mode-locked Quantel YG 402 laser (pulse width 200 ps) was used together with probe assemblies consisting of a 150-W Xe lamp, SPEX minimate monochromator, Hamamatsu R928 NM photomultiplier, and a Biomation 8100 waveform recorder or a Tektronix R7912 digitizer.[75] Digitized signals were averaged and analyzed on a PDP 11/70 computer.[76] Identical results were obtained on all three laser systems. The laser intensity was attenuated with wire-mesh filters (4–100% transmittance) in order to moderate the concentration of the transients. The latter was especially important to test the validity of the second-order kinetics (vide infra). For each experiment, 10 shots were averaged to obtain the decay curves. The kinetics order for the decay was established by a linear least-squares computer fit of the observed decrease of absorbance (A) with time as a function of either ln A or A^{-1} for first and second order, respectively.[17] The kinetics of quenching of the arene radical cations by 9,10-diphenylanthracene and the various pyridine bases were obtained as follows.

Kinetics of Quenching of Methylarene Radical Cations by 9,10-Diphenylanthracene. The quenching of the arene radical cations by DPA was followed subsequent to the CT excitation of solutions containing 0.05 M arene and 0.1 M TNM. The dichloromethane solutions contained 0.1 M tetra-*n*-butylammonium perchlorate and the acetonitrile solutions contained 0.1 M lithium perchlorate. The concentration of DPA was varied from 0.5 to 5 mM. The solutions were excited at 532 nm. The kinetics of the disappearance of arene radical cations were followed at their maximum absorption (e.g., $HMB^{\bullet+}$ at 495 nm; see Table III) and the simultaneous appearance of the radical cation of DPA at 660 nm. Both the kinetics of the disappearance of $ArCH_3^{\bullet+}$ and the appearance of $DPA^{\bullet+}$ followed first-order behavior, and the rate constants were unaffected by the laser-pulse intensity. The rate constants for the electron transfer from DPA to the arene radical cations obtained under pseudo-first-order conditions are listed in Table III.

Kinetics of the Deprotonation of Methylarene Radical Cations by Substituted Pyridine Bases. The kinetics of quenching of the methylarene radical cations by lutidine, collidine, and 2,6-di-*tert*-butylpyridine were followed subsequent to the excitation of solutions containing 0.05 M arene, 0.1 M TNM, and 0.1 M lithium perchlorate in acetonitrile. The concentration of the bases varied from 0.5 to 50 mM. The solutions were excited at 532 nm, and the decay of the radical cations was monitored at the absorption maxima. The decay of the radical cations in the presence of base followed clean first-order kinetics, the rate constants of which were unaffected by variation of the laser-pulse intensity. The rate constants determined under pseudo-first-order conditions (with large excess of base) are listed in Table IV. The kinetic isotope effect for the deprotonation of radical cation of hexamethylbenzene was obtained by following the decay of the cation radicals of HMB and HMB-d_{18} with either pyridine or 2,6-lutidine as the base. All the other decay kinetics were measured in a different laser flash spectrometer as described below.

Effect of Solvent Polarity and Added Salt on the Kinetic Isotope Effect. A detailed study of the effect of solvent polarity on the deprotonation kinetics of the radical cation of HMB (and HMB-d_{18}) was carried out on a laser-flash system consisting of a Quantel YG580-10 Q-switched Nd^{3+}:YAG laser with a pulse width of 10 ns (fwhm). The 1064-nm pulse was frequency doubled with a KDP crystal and separated from the residual 1064 beam with a dichroic mirror to obtain 532-nm pulses of 160–170 mJ per shot. The laser intensity was attenuated with wire-mesh filters (50% and 30% transmittance with energy outputs of 75 and 50 mJ, respectively, at 532 nm). The interrogating beam consisted of the output from a 150-W xenon lamp in an Oriel lamp housing with an Aspherab UV-grade condensing lens. The probe beam was focussed onto the sample, and then the emerging beam from the sample was focussed onto an Oriel 77250 monochromator. A Hamamatsu R928NM photomultiplier tube attached to the exit slit of the monochromator served as the detector. The timing of the sequence for the excitation and probing of the sample was controlled by a Kinetic Instruments sequence generator and laser controller. Data acquisition and digitization were performed with a Tektronix 7104 oscilloscope in conjunction with a Tektronix C101 video camera and Tektronix DCS01 software. The data processing employed an AT&T 6300-plus computer using ASYST 2.0 software. The decay kinetics of the radical cations of HMB and HMB-d_{18} were studied in various solvents. In a typical experiment, 2 mL of a solution containing 0.05 M HMB (HMB-d_{18}) and 0.1 M TNM was placed in a 1-cm quartz fluorimetry cell. The contents were excited at 532 nm, and the decay of the transient signal was followed at 500 nm. In nonpolar solvents such as hexane, benzene, ether, and THF, the decay of the radical cation of HMB (HMB-d_{18}) followed clean first-order kinetics, and the first-order rate constant was not affected by change in the pulse intensity. However, in more polar solvents such as dichloromethane (with and without added salt), nitromethane, acetone, and acetonitrile, the decay of the radical cation appeared more complex. The decay largely followed second-order kinetics (>3 half-lives) accompanied by a possible slow first-order decay. Upon changing the laser-pulse intensity, the second-order rate constant varied ±20%, leading to a ±20% error in the estimation of the rate constants k_2 in Table V. In all the solvent systems studied (with the exception of acetonitrile and a 1:1 (v/v) mixture of acetonitrile and methylene chloride), the decay of the radical cation of HMB-d_{18} was slower than that of HMB. The kinetic isotope effect k_H/k_D, obtained from the second-order rate constants, are listed in Table V for various solvents.

For the study of the salt effect on the kinetic isotope effect, solutions of 0.05 M HMB (HMB-d_{18}) and 0.1 M TNM containing variable

(74) Powell, G.; Johnson, F. R. *Org. Synth.* **1928**, *8*, 92. See also Blackstock, D. J. in ref 5.
(75) Atherton, S. J. *J. Phys. Chem.* **1984**, *88*, 2840.
(76) Foyt, D. C. *J. Comput. Chem.* **1981**, *5*, 49.

amounts of tetra-*n*-butylammonium perchlorate (TBAP) were irradiated at 532 nm with the 10-ns laser pulse. In every case, the decay followed largely second-order kinetics as follows. Salt (M), k_2 (HMB, 10^6 M^{-1} s^{-1}), k_2 (HMB-d_{18}, 10^6 A^{-1} s^{-1}), k_H/k_D: none, 4.3, 1.5, 2.8; 0.008, 0.95, 0.44, 2.1; 0.01, 0.55, 0.34, 1.6; 0.05, 0.40, 0.31, 1.3; 0.10, 0.39, 0.33, 1.2; 0.2, 3.3, 3.1, 1.1 at 25 °C.

General Procedure for the Charge-Transfer Nitration of EDA Complexes. The steady-state photolyses were carried out with a focused beam from either a 1-kW Hg–Xe lamp (Hanovia 977B0010) or a 500-W Hg lamp (Osram HBO 500 W/2). The light beam was passed through a water filter and then through a Corning cutoff filter ($\lambda < 425$ nm, CS-3-72). Irradiation was performed in a 1-cm quartz Schlenck cell immersed in a Pyrex dewar filled with water to maintain the temperature at 25 ± 5 °C. The solution was stirred magnetically throughout the photolysis. After removal of solvent and excess TNM from the photolysate, nitromethane was added as the internal standard for ^{1}H NMR analysis as follows.

Hexamethylbenzene in CH_3CN. Irradiation of a solution containing HMB (48 mg, 0.3 mmol) and TNM (180 μL, 1.5 mmol) in acetonitrile (3 mL) for 2 h using a 1-kW Hg-Xe lamp gave a mixture of (pentamethylphenyl)nitromethane (82%) and (2,2,2-trinitroethyl)pentamethylbenzene (14%). The products were identified by ^{1}H NMR and GC and GC–MS analyses by comparison with those of the authentic samples. An ethereal solution of the reaction mixture was extracted with water, and the amount of nitroform in the aqueous extract was estimated spectrophotometrically.[17,25] The yield of nitroform was 0.23 mmol (80%).

Pentamethylbenzene in CH_3CN. A solution containing PMB (44 mg, 0.3 mmol) and TNM (180 μL, 1.5 mmol) in acetonitrile (3 mL) was irradiated with a 1-kW Hg–Xe lamp for 4 h. Evaporation of solvent and excess TNM gave a yellow oil. ^{1}H NMR and GC analysis indicated the formation of (2,3,4,5-tetramethylphenyl)nitromethane (91%) and nitropentamethylbenzene (6%), which were identified by comparison with authentic samples. The nitroform formed in the reaction was estimated spectrophotometrically as described above for HMB. The yield of nitroform was 0.29 mmol (98%).

Durene in CH_3CN. Photolysis of a solution containing durene (0.04 g, 0.3 mmol) and TNM (180 μL, 1.5 mmol) in acetonitrile for 6 h gave a mixture of (2,4,5-trimethylphenyl)nitromethane (72%) and 3-nitrodurene (21%). The above products were identified by comparison with authentic samples. The GC and GC–MS analyses of the crude product showed the presence of 2,4,5-trimethylbenzaldehyde (5%) and 1-(2′,2′,2′-trinitroethyl)-2,4,5-trimethylbenzene. 2,4,5-Trimethylbenzaldehyde was identified by GC comparison with an authentic sample. The trinitromethylation product was not isolated, but its identification was based on the GC–MS and comparison with the analogous product from hexamethylbenzene. 1-(2′,2′,2′-Trinitroethyl)-2,4,5-trimethylbenzene had a characteristic broad methylene singlet at 4.84 ppm. GC–MS, *m/e* (70 eV): 283 (5, M^+), 238 (9), 160 (10), 159 (10), 146 (10), 145 (26), 144 (14), 133 (28), 132 (31), 119 (20), 117 (29), 115 (20), 105 (15), 91 (28), 77 (15).

Mesitylene in CH_3CN. A mixture of mesitylene (42 μL, 0.3 mmol) and TNM (180 μL, 1.5 mmol) in acetonitrile (3 mL) was photolyzed for 9 h. GC analysis of the crude product with *p*-xylene as the internal standard indicated that the reaction had gone to 70% completion. The yield of 2-nitromesitylene based on the consumption of mesitylene was 65%. GC analysis also indicated the presence of 2,4,6-trimethylbenzoic acid as one of the minor products (<10%).[77] The yield of nitroform, estimated by spectrophotometry, was 56%.

Hexamethylbenzene in CH_2Cl_2. A mixture of hexamethylbenzene (1.0 g, 6.2 mmol) and TNM (1.5 mL, 12.5 mmol) in dichloromethane (20 mL) was photolyzed for 15 h with a 1-kW Hg–Xe lamp. Evaporation of solvent and excess TNM yielded a reddish brown slurry. A portion of the crude product (200 mg) was chromatographed on silica gel. Elution with hexane gave (2,2,2-trinitroethyl)pentamethylbenzene as a pale yellow, crystalline solid: mp 115–117 °C dec. IR (KBr): 3007 (w), 2969 (w), 1603 (s), 1578 (s), 1455 (w), 1428 (w), 1384 (w), 1297 (s), 854 (m), 821 (m), 796 (s) cm^{-1}. ^{1}H NMR ($CDCl_3$): 4.81 (s, br, 2 H, CH_2), 2.23 (s, 3 H, 4-CH_3), 2.19 (s, 6 H), 2.12 (s, 6 H) ppm. MS, *m/e* (solid probe, 70 eV): 311 (M^+, 4) 206 (68), 161 (100), 147 (43). Anal. Calcd for $C_{13}H_{17}N_3O_6$: C, 50.16; H, 5.47; N, 13.50. Found:[78] C, 50.25; H, 5.53; N, 13.43. Elution with benzene gave (pentamethylphenyl)-nitromethane as a colorless, crystalline solid: mp 85–87 °C (lit.[72] mp 86–88 °C). ^{1}H NMR ($CDCl_3$): 5.66 (s, 2 H, CH_2), 2.29 (s, 6 H), 2.25 (s, 9 H) ppm. MS, *m/e* (70 eV): 207 (1, M^+), 162 (14), 161 (100). Further elution of the column with ether, followed by dichloromethane, did not yield any material. Elution with acetonitrile gave a pale yellow, crystalline solid, which was identified as pentamethylbenzyl alcohol by comparison with an authentic sample. Careful analysis of the ^{1}H NMR spectrum of the crude reaction mixture showed the presence of four major products with singlet methylene resonances at 5.77, 5.66, 5.62, and 4.80 ppm. Chromatographic isolation and characterization indicated that the resonances at 5.66 and 4.80 ppm arose from (pentamethylphenyl)nitromethane and (2,2,2-trinitroethyl)pentamethylbenzene, respectively. The other two products with singlet resonances at 5.77 and 5.62 ppm were not isolated from the chromatographic column, presumably due to decomposition on the column. However, they were identified as pentamethylbenzyl nitrite[79] (δ 5.77 ppm) and pentamethylbenzyl nitrate (δ 5.62 ppm) by spectral comparison with authentic samples.

Durene in CH_2Cl_2. Irradiation of a solution containing durene (0.05 M) and TNM (0.1 M) in CH_2Cl_2 (3 mL) gave a mixture of (2,4,5-trimethylphenyl)nitromethane (20%), 3-nitrodurene (20%), 1-(2′,2′,2′-trinitroethyl)-2,4,5-trimethylbenzene (25%), and 2,3,5,6-tetramethylbenzoic acid (5%).[77]

Mesitylene in CH_2Cl_2. Irradiation of a solution containing mesitylene (0.05 M) and TNM (0.1 M) in CH_2Cl_2 (3 mL) gave a mixture of 2-nitromesitylene (40%) and 2,4,6-trimethylbenzoic acid (50%). Both the products were identified by comparison with authentic samples.

HMB in Hexane. Irradiation of a hexane solution (3 mL) of hexamethylbenzene (0.05 M) and TNM (0.1 M) gave a mixture of (pentamethylphenyl)nitromethane (45%), pentamethylbenzyl nitrite (15%), pentamethylbenzyl nitrate (15%), and (2,2,2-trinitroethyl)pentamethylbenzene (20%).[80]

Photolysis of Methylarene EDA Complexes in Acetonitrile Containing Lithium Perchlorate. In a typical procedure, a solution of the arene (0.1 M) and TNM (0.5 M) in acetonitrile containing anhydrous lithium perchlorate (0.1 M) was photolyzed for 6–8 h. After removal of solvent and excess TNM, nitromethane was added (internal standard) and the products were analyzed by ^{1}H NMR. Minor products were analyzed by GC and GC–MS. Hexamethylbenzene gave two major products identified as (pentamethylphenyl)nitromethane (55%) and 1,2-bis(nitromethyl)-3,4,5,6-tetramethylbenzene (26%). The latter was isolated by preparative TLC on silica gel and characterized by ^{1}H and ^{13}C NMR spectroscopy and by its mass spectrum. **1,2-Bis(nitromethyl)-3,4,5,6-tetramethylbenzene.** ^{1}H NMR ($CDCl_3$): 5.82 (s, 4 H, CH_2), 2.37 (s, 6 H), 2.29 (s, 6 H), ppm. ^{13}C NMR ($CDCl_3$): 138.8, 135.8, 126.7, 74.5 (CH_2), 17.4, 16.8 ppm. MS, *m/e* (70 eV): 252 (1, M^+), 206 (13), 177 (13), 176 (100), 175 (89), 161 (71), 160 (88), 148 (95), 147 (88), 145 (82), 133 (59), 130 (25), 129 (35), 128 (32), 117 (17), 115 (30), 105 (24), 91 (34), 79 (13), 77 (24). Both the ^{1}H NMR and ^{13}C NMR spectral data were consistent only with the symmetrical 1,2-disubstituted isomer. A control experiment with (pentamethylphenyl)nitromethane and TNM showed that the same dinitro derivative was formed from the mononitro derivative upon prolonged irradiation.

Pentamethylbenzene gave a mixture of (2,3,4,5-tetramethylphenyl)-nitromethane (50%), nitropentamethylbenzene (19%), 2,3,4,5-tetramethylbenzaldehyde (12%), and 1-(2′,2′,2′-trinitroethyl)-2,3,4,5-tetramethylbenzene (~ 5%, broad singlet at δ 4.89 ppm).

Durene yielded a mixture of (2,4,5-trimethylphenyl)nitromethane (50%), 3-nitrodurene (20%), and 2,4,5-trimethylbenzaldehyde (20%). The trinitromethylation product was present in minor amounts (~5%).

CT Nitration of the EDA Complex from Durene and TNM in the Presence of 2,6-Lutidine. Photolysis of the EDA complex from durene and TNM was carried out in acetonitrile with varying amounts of 2,6-lutidine. In a typical experiment, a solution containing 0.1 M durene and 0.5 M TNM in acetonitrile (3 mL) with 2,6-lutidine (5–100 mM) was irradiated with a 1-kW Hg–Xe lamp and a Corning cutoff filter ($\lambda < 425$ nm CS-3-72). During the photolysis, the solution became an intense yellow and the UV spectrum of the solution indicated a new intense band that overlapped the CT band. After irradiation for 6–8 h, the solvent and excess TNM were removed. The crude product was analyzed by ^{1}H NMR with CH_3NO_2 as the internal standard and also by GC with *p*-xylene as the internal standard. At higher concentrations of base, the reaction did not go to completion. Under these conditions durene gave three major products, (2,4,5-trimethylphenyl)nitromethane, 3-nitrodurene, and 2,4,5-trimethylbenzaldehyde. With increasing concentratons of the base, the yield of 3-nitrodurene decreased and that of 2,4,5-trimethylbenzaldehyde increased. Control experiments showed that both (2,4,5-trimethylphenyl)nitromethane and 2,4,5-trimethylbenzyl nitrate were stable under the experimental conditions. Thus, irradiation of a

(77) Compare: Sankararaman, S.; Kochi, J. K. *Recl. Trav. Chim. Pays-Bas* **1986**, *105*, 278.

(78) Elemental analysis by Atlantic Microlab, Inc., Atlanta, GA.

(79) Compare: (a) Kornblum, N. *Org. React.* **1962**, *12*, 101. (b) Kornblum, N.; Smiley, R. A.; Blackwood, R. K.; Iffland, D. C. *J. Am. Chem. Soc.* **1955**, *77*, 6269.

(80) See: (a) Suzuki, H.; Nakamura K. *Bull. Chem. Soc. Jpn.* **1971**, *44*, 227. (b) Suzuki, H.; Hashihama, M.; Mishina, M. *Bull. Chem. Soc. Jpn.* **1981**, *54*, 1186.

solution containing 0.1 M (2,4,5-trimethylphenyl)nitromethane (or 2,4,5-trimethylbenzyl nitrate), 0.5 M TNM, and 0.1 M 2,6-lutidine in acetonitrile (3 mL) did not lead to any decomposition of the starting material to 2,4,5-trimethylbenzaldehyde. However, 2,4,6-trimethylbenzyl nitrite slowly decomposed at room temperature to give 2,4,5-trimethylbenzaldehyde and reddish brown fumes (NO_2). Thus it is possible that 2,4,5-trimethylbenzaldehyde arose from the decomposition of initially formed 2,4,5-trimethylbenzyl nitrite.[81]

Quantum Yield for Side-Chain Nitration. The quantum yields were measured subsequent to the irradiation of the solution with an Osram 450-W high pressure xenon lamp that was focused through an aqueous IR filter, followed by an interference filter (10-nm bandpass, Edmund Scientific) as a monochromator. A Reinecke salt actinometer was used to calibrate the lamp intensity, as described by Wegner and Adamson.[82] In a typical experiment, 0.05 M arene and excess TNM in 2 mL of acetonitrile was placed in a 1-cm quartz precision cell and irradiated for a given period of time. For hexamethylbenzene and pentamethylbenzene, the quantum yields were measured at 505 nm, and for durene they were measured at 450 nm. The absorbance of the solutions at these wavelengths was always >1.5, and corrections were made for transmitted light. After photolysis, *p*-xylene was added as the internal standard and the side chain nitration products and the unreacted arene were quantitatively analyzed by gas chromatography. The quantum yield for formation of the side chain nitration products and that of the disappearance of the arene were an average of two runs in which the conversions were kept between 5-15%.

(81) Lachowicz, D. R.; Kreuz, K. L. *J. Org. Chem.* **1967**, *32*, 3885.
(82) Wegner, E. E.; Adamson, A. W. *J. Am. Chem. Soc.* **1966**, *88*, 394.

Acknowledgment. We thank the National Science Foundation and the Robert A. Welch Foundation for financial support. J. M.M. also gratefully acknowledges support from SOHIO, the Cleveland State College of Graduate Studies, and the donors of the Petroleum Research Fund, administered by the American Chemical Society. We thank M. A. J. Rodgers, S. J. Atherton, and the Center for Fast Kinetics Research [under support from the National Institute of Health (Grant No. RR 00886) and the University of Texas at Austin] for use of their laser facilities and the National Science Foundation for the funds to construct a laser-flash system in Houston. We also acknowledge the participation of T. Lund (U.H.) in the early stages of this study.

Intramolecular Dissociative Isomerization and the Presence of Trans Influence in 12-Sb-6 Ate Complexes and Their Protonolysis[1,2]

Yohsuke Yamamoto, Hisao Fujikawa, Hiroshi Fujishima, and Kin-ya Akiba*

Contribution from the Department of Chemistry, Faculty of Science, Hiroshima University, Higashisenda-machi, Hiroshima 730, Japan. *Received August 17, 1988*

Abstract: The reaction of methyllithium with 3,3-bis(trifluoromethyl)-1,1,1-tris(*p*-methylphenyl)-3*H*-2,1-benzoxastilbole (10-Sb-5, **2a**) gave a 12-Sb-6 ate complex (**5a**). At −78 °C a single isomer (**5aA**) with the methyl group cis to the oxygen atom was formed. ^{19}F NMR of **5aA** showed a pair of quartets, indicating the presence of nonequivalent CF_3 groups. When the solution was warmed to room temperature, equilibration took place among three positional isomers, **5aA**, **5aB**, and **5aC**, and resulted in the ratio of 61:23:16 at 20 °C, respectively. The mechanism for the isomerization was concluded to be an intramolecular dissociation involving cleavage of an endocyclic Sb–O bond and pseudorotation of the resulting 10-Sb-5 intermediate. The mechanism was supported by kinetic measurements of the isomerization with or without HMPA (12-crown-4) and of quenching with **5a** with EtOH. Trans influence of the oxygen atom on the equilibrium ratio of the mixture of **5b**, which was generated by the reaction of *p*-$CF_3C_6H_4Li$ with **2a**, was observed. Ab initio calculation was carried out on model compounds H_5SbF^-, H_5SbOH^-, and $H_4SbF_2^-$ to support the electron-withdrawing effect of the electronegative atom on the trans hydrogen. Protonolysis of 12-Sb-6 (**5**) ate complexes was concluded to take place by the initial protonolysis at the oxygen atom to form zwitterion (**5**–H^+) which is followed by ring-opening to pentacoordinated antimony (**8**). A hydrocarbon is eliminated from **5**–H^+ during rapid equilibration between **5**–H^+ and **8**.

The synthesis, structure, and reaction of hypervalent compounds of main-group elements below the second row have been attracting increasing interest, and several successful reports for synthesizing those of the first row have recently expanded this area of chemistry.[3] Hypervalent compounds of the former class have shown characteristic features based on the essentially weak and polarizable nature of the hypervalent bond. Recently, Barton et al. reported extensive work on phenylation of enols, phenols, and amines by the use of 10-Bi-5 compounds.[4] We recently reported selective reductive coupling of two ligands, dehydrogenation of benzoins, and some other reactions using acyclic pentacoordinate antimony compounds and revealed rather unique characteristics of them.[5] Then we paid our attention to hexacoordinate antimony ate complexes, which were known to be unstable,[6] and only one

(1) For a preliminary account of a part of these results, see: Akiba, K-y.; Fujikawa, H.; Sunaguchi, Y.; Yamamoto, Y. *J. Am. Chem. Soc.* **1987**, *109*, 1245.
(2) The *N*-X-*L* designation was proposed previously: X, central atom; *N*, formal valence-shell electrons about an X; *L*, the number of ligands. See: Perkins, C. W.; Martin, J. C.; Arduengo, A. J.; Lau, W.; Algeria, A.; Kochi, J. K. *J. Am. Chem. Soc.* **1980**, *102*, 7753.
(3) 10-C-5: Forbus, T. R.; Martin, J. C. *J. Am. Chem. Soc.* **1979**, *101*, 5057. 10-B-5 and 12-B-6: Lee, D. Y.; Martin, J. C. *J. Am. Chem. Soc.* **1984**, *106*, 5745. 10-F-2: Farnham, W. B. *Chem. Eng. News* **1986**, June 2, 22.
(4) Phenols and enols: Barton, D. H. R.; Finet, J.-P.; Khamsi, J.; Pichon, C. *Tetrahedron Lett.* **1986**, *27*, 3619, and references there cited. Amines: Barton, D. H. R.; Finet, J.-P.; Khamsi, J. *Tetrahedron Lett.* **1987**, *28*, 887, and references there cited.
(5) Akiba, K-y.; Shimizu, A.; Ohnari, H.; Ohkata, K. *Tetrahedron Lett.* **1985**, *26*, 3211. Akiba, K.-y.; Ohnari, H.; Ohkata, K. *Chem. Lett.* **1985**, 1577. Ohkata, K.; Ohnari, H.; Akiba, K-y. *J. Chem. Soc. Jpn.* **1987**, 1267. Akiba, K-y.; Okinaka, T.; Nakatani, M.; Yamamoto, Y. *Tetrahedron Lett.* **1987**, *28*, 3367. Yamamoto, Y.; Okinaka, T.; Nakatani, M.; Akiba, K-y. *J. Chem. Soc. Jpn.* **1987**, 1286.
(6) Hellwinkel, D. *Top. Curr. Chem.* **1983**, *109*, 1. *Gmelin Handbook of Inorganic Chemistry, 8th Ed; Sb Organoantimony Compounds*; Wieber, M., Ed.; Springer-Verlag: Berlin, 1985; Part 3, p 1.

0002-7863/89/1511-2276$01.50/0